



A review on 2D transition metal di-chalcogenides and metal oxide nanostructures based NO₂ gas sensors



Sunil Kumar ^{a,d,*}, Vladimir Pavelyev ^a, Prabhash Mishra ^{a,b,c}, Nishant Tripathi ^a, Prachi Sharma ^a, Fernando Calle ^d

^a Department of Nanoengineering, Samara National Research University, 34, Moskovskoye shosse, Samara, 443086, Russia

^b Center for Photonics and 2D Materials, Moscow Institute of Physics and Technology (MIPT), Dolgoprudny, 141700, Russia

^c Centre for Nanoscience and Nanotechnology, Jamia Millia Islamia (A Central University), Jamia Nagar, New Delhi, 110025, India

^d ISOM and Dep. Ingeniería Electrónica, E.T.S.I. Telecomunicación, Universidad Politécnica de Madrid, Av. Complutense 30, Madrid, 28040, Spain

ARTICLE INFO

Keywords:
2D materials
Metal oxide
NO₂
Gas sensors
TMDs

ABSTRACT

NO₂, having a reddish-brown color and biting odor, is the most prominent toxic waste present in the atmosphere. The major contributors to NO₂ gas include emissions from industrial and transport sectors. There are many porous nanostructures which have shown enormous potential for NO₂ gas sensing. Among these, the first group comprises metal oxides while the second group includes two-dimensional transition metal dichalcogenides (2D TMDs). Besides, these materials have also been modified or functionalized with different metals for improving various sensing parameters such as selectivity, sensitivity, affordability, stability and life span of the device. In this article, we discuss new developments in the fields of metal oxide nanostructures and 2D TMDs for NO₂ sensing. Additionally, a comparative analysis of different modifications and their effects on sensing properties of both the materials is presented.

1. Introduction

According to a 2018 report of the World Health Organization (WHO), air pollution is one of the major environmental risks to health. Diseases like stroke and cancer are killing millions of people every year owing to inhalation of microscopic pollutants present in the air, which can easily penetrate into the circulatory and respiratory systems, damaging heart, brain, and lungs. According to this report, the majority of the world's population is living in places where WHO air quality guidelines are not met [1]. The major contributors to deteriorating air are nitrogen oxides (NO_x) such as nitrogen dioxide (NO₂) and nitrogen oxide (NO) [2]. Anthropogenic activities, especially combustion practices are responsible for the presence of the most prevalent and toxic form of NO_x gases, i.e. NO₂ in the atmosphere. Excessive exposure to NO₂ has adverse effects on both human and wildlife. The trace amount detection of NO₂ in the medical field is highly desirable because of its ability to give fingerprints for chronic obstructive pulmonary disease (COPD). The indoor threshold limit value (TLV) for NO₂ as stated by occupational safety and health administration is 5 ppm. Besides, the long term (LTEV) and short term exposure (STEV) values for NO₂ are 3

and 5 ppm, respectively, as stated by ACGIH (American Conference of Governmental Industrial Hygienists is also known as Association Advancing Occupational and Environmental Health) [3]. In the modern world, with the abrupt rise of industry and rapid increments in the number of automobiles, NO₂ has become a major contributor to pollution. NO₂ is also responsible for the formation of acid rain and ozone-depleting substances emitted through human activities [4–7]. And it raises the demands for NO₂ detectors.

Over the past decades, extensive work has been done on metal oxide-based NO₂ gas sensors. The presence of active sites on the surface of metal oxides is responsible for their gas sensing properties. Thus, the gas sensing mechanism mainly depends on the amount of crystallinity, particle size and the number of defects present in metal oxide nanostructures. Different nanostructures of metal oxides such as nanorods, nanoparticles and nanoflowers, have been used in NO₂ gas sensor fabrication because of their inherent properties like low cost, high chemical and thermal stabilities, nontoxicity and high chemical sensitivities which are attributed to the presence of high-density free charge carriers [8]. The low surface area of bulk silicon makes it's unsuitable for sensing applications. However, metal-assisted chemical etching method

* Corresponding author. Department of Nanoengineering, Samara National Research University, 34, Moskovskoye shosse, Samara, 443086, Russia.
E-mail address: sunil.kr.rai@outlook.com (S. Kumar).

is used for obtaining porous silicon which shows fast response and selectivity towards NO_2 [9].

The mechanism of resistive NO_2 gas sensing based on metal oxides and TMDs is as follows: an electronic device whose electrical resistance is a function of ambient gas concentration is generally used as a resistive gas sensor. The detection of various ambient gases with variations of their concentration is particularly achieved by resistive gas sensors. The main part of the sensor is an active layer. The active layer can be made up of various materials which could be organic, inorganic or a hybrid combination of the two. The function of transducers is to convert variations in chemical interactions (i.e., electrostatic interactions, the formation of H-bonds, etc.) to a measurable signal (electrical, optical, etc.) or physical property (i.e., conductivity, refractive index, etc.) corresponding to gas concentration [10–13]. Several mechanisms are involved in a gas sensor operation such as sensing and transduction (optical, electrochemical, capacitive, resistive, etc.). However, the main disadvantage of the resistive gas sensors includes limited sensitivity and poor or no selectivity. Various strategies have been employed to overcome these shortcomings, e.g. formation of porous sensing layers, varying the operating temperature of the sensor, etc. [14].

In the beginning, the fascinating properties of graphene and its derivatives attracted researchers to develop NO_2 detector based on them, but the absence of an electronic bandgap in graphene has forced researchers to find some alternative elements such as 2D materials with semiconducting properties. In this process, transition metals di-chalcogenides (TMDs) being semiconducting in nature and an MX_2 structure, where 'M' stands for transition metal atoms (such as W, Mo, Ti, Ta) and 'X' stands for a chalcogen atom (such as S, Se, Te). The robustness of MoS_2 makes it the most studied TMD material. The use of TMD materials in fields such as flexible electronics, optoelectronics, high-end electronics, energy harvesting, personalized medicine, spin-orbit coupling, a unique combination of atomic-scale thickness, favourable electronic and mechanical properties and direct bandgap structure [15–21].

With progress in nanotechnology over the years, significant progress has been made in sensing technology with conducting polymers, carbon nanotubes and 2D materials and oxide nanostructures. Nowadays, in materials engineering, the use of transition metals di-chalcogenides (TMDs) and metal oxides has become the most impressive way for improving the performance of solid-state materials based gas sensors. The use of metal oxides and TMDs is known to improve the selectivity, sensitivity, response and repeatability, of gas sensors [22–24]. Many solid-state gas sensors have been developed for detecting different toxic gases. Among these transition metals di-chalcogenides (TMDs) and metal oxides based chemiresistive gas sensors are quite promising. These sensors have low response time, high sensitivity, selectivity, cost-effective and great suitability for the design of movable apparatus. These unique properties make the sensor more suitable for advanced applications like an artificial nose, portable instruments and alarm systems [25,26].

Several strategies have been employed to enhance the performance of metal oxide-based sensors such as (1) one dimensional metal oxide nanostructures show improved thermal stability; (2) surface modification of noble metals is known to improve the response-recovery kinetics and sensitivity of the overall device; and (3) the morphology of deposit films and catalytic reactivity can be modified by doping the metal oxides with transition metals [27–30]. In recent years, nanostructured metal oxides have attracted huge attention to their application in NO_2 gas sensors [31–36].

The mechanism behind enhancement in sensor response can be attributed to the modulation behaviour of p-n junction as well as the contact resistances. The total variation in sensor resistance during molecule desorption/adsorption processes could be ascribed to occupation modulation of sorption sites and periodic tailoring of p-n junctions. For example, when n-type MoS_2 is exposed to air, the surface

adsorbed oxygen will capture electrons from the conduction band to generate oxygen anions (O_2^-), resulting in the formation of an electron shell depletion region (EDR) on the surface. Hence, this procedure leads to an n-type semiconducting core region as low resistance and EDR as high resistance regions. In the case of p-type semiconductors, the adsorbed oxygen anions from the hole accumulation region (HAR) as a low resistance region near the material surface because of the electrostatic interaction between oppositely charged species. Prior to NO_2 gas exposure, p-n junction results in an extension of charge depletion layer by recombination of electrons and holes. Considering that molecular NO_2 adsorption proceeds in the form of NO_2^- via continuous electron withdrawal from rGO or MoS_2 , both HAR and EDR would be extended, accompanying a negative and positive impact on the resistance increase, respectively. However, upon exposure to NO_2 gas, the effect of HAR on total resistance change dominates over EDR, thereby leading to a net decrease of overall resistance [37,38]. This effect can be ascribed to more reluctance in MoS_2 to its resistance change than rGO.

The advancements in the material engineering for achieving the optimum performance or even possibly achieve new function for feasible utilization involve hybridization of two or more materials, which is the most interesting progress to vanquish the flaws of a particular material [39,40]. The recent success to use scalable techniques and solution precessing for preparing 2D TMDs nanosheets has created a great opportunity for developing functional composite nanostructures by exploiting them as building blocks [41]. In the last ten years, most of the studies have focused on the construction of functional composites of reduced graphene oxide (rGO) and graphene oxide (GO) for various applications. Success in the development of graphene-based nanostructures has inspired many researchers to explore various ways of incorporating ultrathin layers of TMDs in different materials [42–47]. Generally, the research based on TMDs is concentrated on: (1) the assembly or synthesis of TMD sheets of hierarchical nanostructures, (2) layered composites of TMD nanostructures, (3) developing in-plane doped or 2D alloyed heterostructures.

In the last decade, NO_2 sensor development has been reviewed by numerous researchers based on a diverse range of materials, i.e., metal oxide nanoparticles, 2D materials like MoS_2 , carbon nanotubes [48–53], nanowires [54,55], polymers [56,57], and so on. The progress of the NO_2 gas sensor can be analyzed by the number of scientific publications in the last decade as shown in Fig. 1. In this review, our aspiration is to provide a summary and comprehensive study of the promptly rising research direction and broad perspective of the crucial challenges, prospects and knowledge in this encouraging area of NO_2 gas sensors. The gas sensors on NO_2 have been developed based on many materials and hybrid structures, but here our focus will be on NO_2 gas sensors on 2D TMDs and metal oxide-based nanostructures. The progress in various

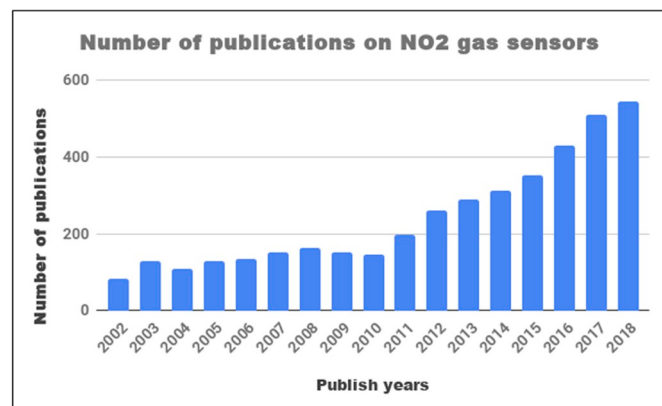


Fig. 1. The number of publications on NO_2 gas sensors from 2002 to 2018 (internet search of the web of science on 1st January 2019). Keywords for search: NO_2 gas sensor.

characteristics such as structure, method of preparation, concentration, sensitivity, operating temperature and recovery and response time for NO₂ gas sensors based on 2D-TMDs and hybrid structure is summarized in Table 1. Table 2 shows a comparison of various sensor parameters for NO₂ gas sensors developed from metal oxides and their composites.

2. Materials for NO₂ gas sensors

2.1. 2D transition metal dichalcogenides (TMDs)

TMDs, having an ultrathin thickness and 2D morphology, present some exceptional chemical, electrical and physical properties as compared with their bulk equivalent and hence carry an immense assurance for diverse applications [20,58–61]. There are many methods employed to prepare one or few-layered TMD nanosheets, such as chemical vapor deposition (CVD) process, liquid-phase exfoliation, wet chemical synthesis, mechanical cleavage method and electrochemical exfoliation using Li-intercalation [62–66]. The electrical and chemical properties of 2D nanostructures have made them relevant for their use in numerous applications, e.g., sensors, electronic/optoelectronic apparatus, energy storage and electrolysis [67–77]. Some structural properties of TMDs are similar to graphene. In addition to this, they exhibit some complementary properties and features which make them suitable for sensing applications. A typical example is the fabrication of electronic transistors. Although at room temperature graphene has remarkably high carrier mobility, it has poorly defined bandgap, which makes it difficult to turn off the transistors. Clearly, graphene in its pristine form is not suitable for fabricating logic gates. On the contrary, many TMDs (such as MoS₂, MoTe₂ and WS₂) depict semiconducting behaviour, have a wide range of bandgap and are better suited for their use as electronic devices.

2.1.1. MoS₂ based NO₂ gas sensors

Among all TMDs materials, MoS₂ has got special attention for gas sensing applications. Its layered structure, high surface to volume ratio, scalability, high yield production, and cost-effectiveness make it special for gas sensing. The liquid exfoliation technique is emerging as an excellent approach for the synthesis of single or few-layered MoS₂. Furthermore, it is inherently suited for gas sensing applications owing to the introduction of a significant concentration of S vacancies in MoS₂ basal plane, which can be either functionalized via substitutional doping or behave as adsorption sites for target gases. N-Methyl Pyrrolidone

(NMP) has emerged as the most suitable solvent to effectively exfoliate MoS₂. Also, MoS₂ is a natural reservoir of N atoms that can potentially dope the solute if the system is heated in the 150–200 °C temperature range and it can also play the role of doping agent, allowing to finely tune the response of MoS₂ to target gases [78,79].

MoS₂ has exceptional sensing properties but it also shows some limitations. A most serious issue with MoS₂ based sensor is its stability which is caused by fast oxidation of its top layer. MoS₂ is readily oxidized to MoO₃, which decreases the sensitivity. In order to counter the oxidation problem, Lingmin et al. made hierarchical MoS₂ spheres like a 3D flower for NO₂ sensing (see Fig. 2(a) and (b) and (c)) [15]. They reported that MoS₂ flowers can remain stable for a long time as compared to MoS₂ films. Another advantage of using MoS₂ flowers is their porous nature which enhances the surface area and also provides additional channels for gas molecule absorption. The BET surface area of spheres like a 3D flower was found to be around 27.7 m²/g (see Fig. 2(d)). The gas detection of as-developed flower-like MoS₂ for 50 ppm of NO₂ was done in variable temperature conditions (from 100 to 250 °C) to attain the optimum operating temperature. It was found that the maximum response of 78% was obtained at a temperature of 150 °C as depicted in Fig. 3(a). The MoS₂ sensor response curve towards NO₂ of 50 ppm is shown in Fig. 3(b) which shows that as-developed MoS₂ spheres act as a p-type semiconductor. The p-type behaviour is attributed to a reduction in sensor resistance on exposure to NO₂, where NO₂ behaves as the oxidizing gas. The dynamic sensing response of the sensor for various concentrations of NO₂ (5–50 ppm) is depicted in Fig. 3(c), showing an increase in the sensitivity with increasing concentration of NO₂. The sensitivity and selectivity of the sensor for various gases are demonstrated in Fig. 3(d). Fig. 3(e) demonstrates good repeatability of the sensor response. The stability of the MoS₂ spheres like a 3D flower was checked for various days and the results as depicted in Fig. 3(f) indicate the high stability of the sensor. The adsorption of NO₂ as oxidizing gas molecules on the surface of MoS₂ led to large p-type doping of MoS₂, which significantly increases the conductance of MoS₂ [80,81].

A unique technique was developed by Zeng et al., in which the surface morphology of the developed MoS₂ was tailored by changing the concentration of cetyltrimethyl ammonium bromide (CTAB) during hydrothermal treatment [17]. The hierarchical porous microspheres of MoS₂ exhibited good response and recovery properties along with high selectivity and reversibility. CTAB was found to play a very important role in deciding the morphology of resulting MoS₂. An increase in the

Table 1
NO₂ gas sensors based on 2D transition metal di-chalcogenides (TMDs).

| Sl. no | Method of preparation | Structure | Materials | Concentration | Response time/Recovery time | Response | Operating temperature (°C) | References |
|--------|------------------------|--------------------|------------------------------------|---------------|-----------------------------|----------|------------------------------------|------------|
| 1. | Hydrothermal | 3D flower | MoS ₂ | 50 ppm | —/— | 78% | 150 | [15] |
| 2. | Aerogel conductometric | Composite | WS ₂ /GA | 2 ppm | 100 s/300 s | 3% | 180 | [16] |
| 3. | Hydrothermal-CTAB | 3D flower | MoS ₂ | 50 ppm | —/— | 60% | 100 | [17] |
| 4. | Sulphurisation | Vertically aligned | MoS ₂ /ZnO NWs | 50 ppm | 5 min/- | 31.2% | 200 | [19] |
| 5. | Hydrothermal | Nanosheets | WS ₂ | 0.1 ppm | —/— | 9.3% | RT | [59] |
| 6. | Wet chemical | Hybrid | MoS ₂ -RGO | 3 ppm | 8 s/20 s | 1.23 | 160 | [60] |
| 7. | Hydrothermal | Hollow | MoS ₂ | 100 ppm | 79 s/225 s | 40.3% | 150 | [61] |
| 8. | Two-step CVD | Bilayer | MoS ₂ | 1 ppm | 11.3/5.3 min | 2.6% | RT | [86] |
| 9. | Solvochemical | Nanocomposite | RGO-MoS ₂ -CdS | 0.2 ppm | 25 s/34 s | 27.4% | 75 | [89] |
| 10. | CVD | Monolayer | MoS ₂ | 400 ppb | 16 s/65 s | 670% | RT (625 nm, 4 mW/cm ²) | [90] |
| 11. | CVD | Nanowires | MoS ₂ | 5 ppm | 16 s/172 s | 18.1% | 60 | [92] |
| 12. | Redox reaction | Nanoparticle | MoS ₂ -Au | 2.5 ppm | 4/14 min | 30% | RT | [93] |
| 13. | Annealing | Nanocomposite | NiO/WO ₃ | 30 ppm | 2.5 s/1.1 s | 4.8 | RT | [109] |
| 14. | Electrospinning | Nanofiber | WS ₂ @MTCNFs | 1 ppm | 3.73 min/- | 15% | RT | [146] |
| 15. | Chemical etching + CVD | Nanosheet | MoS ₂ /PSi NWs | 50 ppm | —/— | 28.4% | RT | [147] |
| 16. | Wet chemical | Nanostructure | MoS ₂ /ZnO | 5 ppm | 40 s/1000 s | 3050% | RT | [95] |
| 17. | Nucleation controlled | Microflowers | MoS ₂ -MoO ₃ | 10 ppm | ~19 s/~182 s | 33.6% | RT | [97] |
| 18. | CVD | flakes | VA-MoS ₂ | 50 ppm | —/— | 48.32% | 100 | [98] |

Table 2NO₂ gas sensors based on Metal-oxide based nanostructures.

| Sl. no | Method of preparation | Structure | Materials | Concentration | Response time/ Recovery time | Response | Operating temperature (°C) | References |
|--------|-------------------------------------|-----------------------------|--------------------------------------|---------------|---------------------------------|-------------------------|-------------------------------------|------------|
| 1. | Facile solvothermal | Microspheres | ZnO/SnO ₂ | 100 ppm | ~33 s/~7 s | 258 | 200 | [31] |
| 2. | Spray deposition | Heterojunction | ZnO/m-SWCNT | 10 ppm | 74 s/- | | RT | [148] |
| 3. | Surface etching | Microwire (MW) | ZnO | 10–50 ppm | 221 s/118 s | ~411% | – | [33] |
| 4. | Facile two-step synthesis | Actinomorphic flower | ZnO/ZnFe ₂ O ₄ | 0.1 ppm | 7 s/15 s | 250 | 200 | [34] |
| 5. | Hydrothermal | Silk Fibroin (SF) | ZnO/SF | 20 ppm | 26 s/16 s | 85 | RT | [35] |
| 6. | Drop casting | Heterostructures | Silicon/ZnO | 200 ppb | 50 s/- | 35% | 25 | [36] |
| 7. | Modified polymer-network gel method | Heterostructures | ZnO-Ag | 0.5–5 ppm | ~250 s/~200 s | 1.545 ppm ⁻¹ | RT (470 nm/75 mW/cm ²) | [120] |
| 8. | Thermal reduction | Nanosheets | ZnO/rGO | 50 ppm | 25 s/15 s | 9.61 | RT | [121] |
| 9. | Facile Hydrothermal | Nanowire | ZnO | 1–30 ppm | 25 s/21 s | 3.3 | 250 | [110] |
| 10. | Facile three-step process | Nanowire | ZnO-CuO | 10 ppm | ~400 s/~300 s | 48.4 | 350 | [111] |
| 11. | Thermal evaporation | Heterostructure | ZnO/CuO | 100 ppm | 14 s/197 s | 175% | 150 | [119] |
| 12. | Sol-gel spin coating | Thin film | ZnO | 100 ppm | 3 s/137 s | 12.3 | 200 | [124] |
| 13. | Thermal evaporation | Nanorods | ZnO | 100 ppm | 35 s/206 s | 622 | 200 | [54] |
| 14. | Thermal evaporation | Nanowires | ZnO | 100 ppm | 17 s/290 s | 101 | 200 | [54] |
| 15. | Facile Two-step Hydrothermal | Hierarchical nanostructures | SnO ₂ @ZnO | 5 ppb | 60 s/45 s | 0.2 | 150 | [55] |
| 16. | Electrospinning | Nanowebs | SnO ₂ -NiO | 1,5,10 ppm | 330,173,163 s/261,301,204 s | 10.5,22.8, 36 | 300 | [149] |
| 17. | Oil bath precipitation | Brick-like | In ₂ O ₃ | 500 ppb | 114 s/49 s | 402 | 50 | [132] |
| 18. | Precipitation-calcination | Mesoporous sheets | ZnO | 1 ppm | 3/2.5 min | 130% | RT | [129] |
| 19. | Hydrothermal | Nanowires | Pd-ZnO | 1 ppm | 141 s/177 s | 13.5 | 100 | [28] |
| 20. | Thermal reduction | Nanowalls | ZnO/rGO | 50 ppm | ~37 s/2 s | 35.31 | RT (365 nm/1.2 mW/cm ²) | [112] |
| 21. | Thermal annealing | Film | ZnO/rGO | 100 ppm | 6.2/15.5 min | 47.4% | RT | [150] |
| 22. | Sol-gel spin coating | Thin film | Al:ZnO | 100 ppm | 8 s/121 s | 18.5 | 200 | [151] |
| 23. | Hydrothermal | Nanowire | Au-ZnO | 1 ppm | 29 s/18 s | 31.4 | 150 | [116] |
| 24. | Sol-gel | Thin film | G-ZnO | 5 ppm | 150 s/315 s | 894% | 150 | [152] |
| 25. | OFET | Nanostructure | P3HT-ZnO@GO | 1,5 ppm | –/– | 32,210% | RT | [125] |
| 26. | Microwave assisted hydrothermal | Hollow spheres | ZnO-BP | 1 ppb | 2 s/16 s | 130.7% | RT | [126] |
| 27. | Brush coating | Nanoparticles | ZnO | 234 ppm | 2 s/20 s | 275% | 280 | [153] |
| 28. | Thermal evaporation and sol-gel | Nanorods | Pd/ZnO-SnO ₂ | 5 ppm | 17.74 s/60 s | 5.52 | 300 | [130] |
| 29. | Wet chemical and refluxing | Nanochains | CuO-ZnO/rGO | 40 ppm | 40 s/- | 62.9% | RT | [131] |
| 30. | Soft chemical synthetic | Flower shaped thin film | ZnO | 10 ppm | 65 s/54 s | 55 | 200 | [32] |

concentration of CTAB was observed to create different shapes such as flowers, sheets and spheres. The perfect 3D spherical morphology of MoS₂ was obtained at an optimum concentration of 6 g/L. The process of adsorption and desorption of oxygen molecules on the surface of MoS₂ is responsible for gas sensing properties of the hierarchical 3D flower-like MoS₂ nanospheres. MoS₂ acts as n-type semiconductors such that in the presence of air, oxygen molecules adsorb on the surface of MoS₂ nanospheres and form ionic species (O²⁻, O⁻, O²⁻) by capturing free electrons from the conduction band of MoS₂. This results in a decrease in the electrical conductivity or an increase in the resistance of the sensor. Oxidizing gases such as NO₂ with higher electrophilic properties capture electrons of MoS₂. Further, NO₂ also reacts with adsorbed oxygen ions to form NO₂⁻. Hence the resistance of the gas sensor increases on exposure to NO₂. The authors achieved better gas sensing response in this work than some of the hybrid gas sensors as reported in Refs. [15,58,82].

The surface area can be improved in a hybrid structure. In this context, Bon-Cheol fabricated an extremely stretchable and transparent NO₂ gas detecting thin films using soft lithographic patterning on MoS₂-rGO composites [18]. A facile solution mixing process was used for preparing the MoS₂-rGO composite thin films. The composite thin film was spin-coated on the surface of the substrate followed by annealing in N₂ atmosphere for 1 h. A soft lithography technique was used for line patterning of hydrothermally reduced GO (rGO), and the MoS₂-rGO patterned composite thin films were again transferred on a PET substrate. The complete fabrication and patterning of MoS₂-rGO composite thin film are depicted in Fig. 4. The MoS₂-rGO composite was prepared

by mixing various concentrations of both MoS₂ and rGO. Sensing properties of different sensors with changing concentrations of both MoS₂ and rGO are shown in Fig. 5. In comparison with pure rGO sensor, the sensitivity of MoS₂-rGO composite thin film towards NO₂ was 4 times higher. The electric characteristics of the MoS₂-rGO composite film sensor were maintained even when the sensor was bend about 70%. In comparison with pure rGO films, the sensitivity of the gas sensor developed on MoS₂-rGO composite film was found to be at least 300% more.

Another way of obtaining a large surface area for a gas sensor is the development of vertically aligned nanostructures. Zhengcao et al. achieved highly enhanced NO₂ gas sensing performance using vertically aligned MoS₂/ZnO nanowires in the year 2018 [19]. The vertically aligned structure of MoS₂ nanosheets was produced by sulphurisation of Mo films predeposited by magnetic sputtering on hydrothermally synthesized ZnO nanowires. The dynamic response of the MoS₂-ZnO NWs sensor measured for 50 ppm of NO₂ gas with varying temperature is demonstrated in Fig. 6(a). It can be seen that the sensor repeatability at RT and 100 °C was zero while the sensor recovers 70–100% at 200 °C. This observation was also found for graphene-based sensors [83] and also in MoS₂ based sensors [84]. The sensing response as a function of gas concentration is depicted in Fig. 6(b). According to the response and recovery curves, the optimum operating temperature was found to be 200 °C. The comparative sensing response of pure MoS₂, ZnO NWs and MoS₂/ZnO nanowires at 200 °C is exhibited in Fig. 6(c). It was found that the sensing response of MoS₂/ZnO nanowires is superior to that of

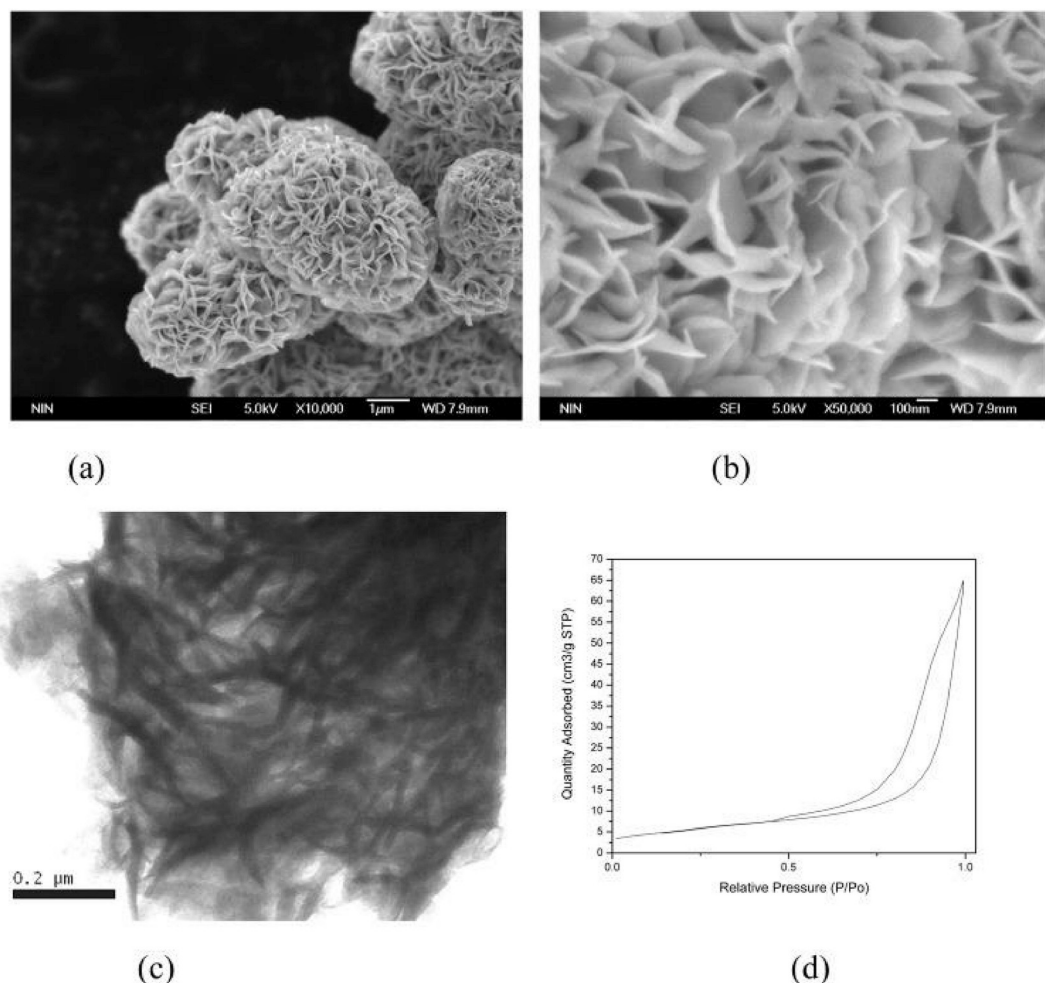


Fig. 2. (a) Low magnification SEM images of as-prepared MoS₂ spheres like 3D flower, (b) High magnification SEM photograph, (c) TEM photograph, (d) BET photograph. Copyright permission from Ref. [15].

both MoS₂ and ZnO NWs. The response and repeatability of the MoS₂/ZnO nanowires sensor towards 50 ppm NO₂ are demonstrated in Fig. 6(d). The results show that in comparison to as-processed MoS₂ and ZnO NWs, the MoS₂/ZnO nanosheets demonstrated outstanding repeatability, recovery, selectivity, sensitivity, as a function of working temperature and also efficient to detect as low as 200 ppb of NO₂ gas.

Donarelli et al. presented another way of changing the semiconducting behaviour of MoS₂ flakes by changing the annealing temperature. The chemically exfoliated MoS₂ based gas detector response was examined in the presence of NO₂ and other gases [20]. The chemical exfoliation of MoS₂ flakes was carried out in N-methyl pyrrolidone (NMP) followed by annealing at 150 °C or 250 °C in air. The formation of percolation paths in MoS₂ flakes as a result of interconnection between the sensing device and the electrodes is revealed by SEM analysis of the exfoliated MoS₂ flakes. The crystalline nature of the MoS₂ flakes before annealing confirmed by Raman spectroscopy while there were no appreciable bulk impurities in MoO₃ after annealing. Under the exposure of NO₂ gas, the detector processed with thermal annealing displayed a unique response of p-type. This behaviour can be attributed to nitrogen doping of "s" vacancies in MoS₂ surface, where the nitrogen atoms are possibly contributed by NMP during chemical exfoliation. The thermal annealing of sensor exhibits the n-type behaviour under exposure of NO₂. This behaviour can be attributed to significant existence of "s" vacancies in MoS₂ annealed flakes and to the surface coexistence of MoO₃ arising from the limited chemical exfoliation of the surface of the flake.

Yong's group, in 2017, developed a unique way of p-n junction tailoring and occupation modulation of sorption sites of rGO-MoS₂ nanocomposite for ultrasensitive sensing of NO₂ gas at a low operational temperature [58]. In his article, both rGO and rGO-MoS₂ hybrid thin-film sensors were fabricated for the detection of NO₂ gas at low operating temperature. The electrical response of both rGO and rGO-/MoS₂ composite sensors exhibited p-type characteristic response as demonstrated in Fig. 7(a and b). The characteristic response of the rGO sensor is p-type because of the presence of oxygen and water doping [85]. The periodic tailoring of the p-n junction and occupation modulation of sorption sites can be attributed to the total resistance variation of the rGO-MoS₂ sensor during molecular desorption/adsorption process. When n-type MoS₂ is exposed to air, the surface adsorbed oxygen will capture electrons from its conduction band to generate oxygen anions (O₂⁻), resulting in the formation of electron shell depletion region (EDR) on the surface. This results in the formation of the n-type semiconducting core region with low resistance and EDR with high resistance. Similarly, in the case of p-type semiconductors, the adsorbed oxygen anions from the hole accumulation region (HAR) with low resistance near the material surface owing to electrostatic interaction between oppositely charged species. The formation of p-n junction leads to an increase in the width of the space charge layer resulting in enhancement of sensor response and it is expected for rGO-MoS₂ junctions. The adsorption of NO₂ gas molecules creates NO₂⁻ through continuous recombinations from both MoS₂ and rGO. Hence both EDR and HAR would be continued, followed with both positive and negative

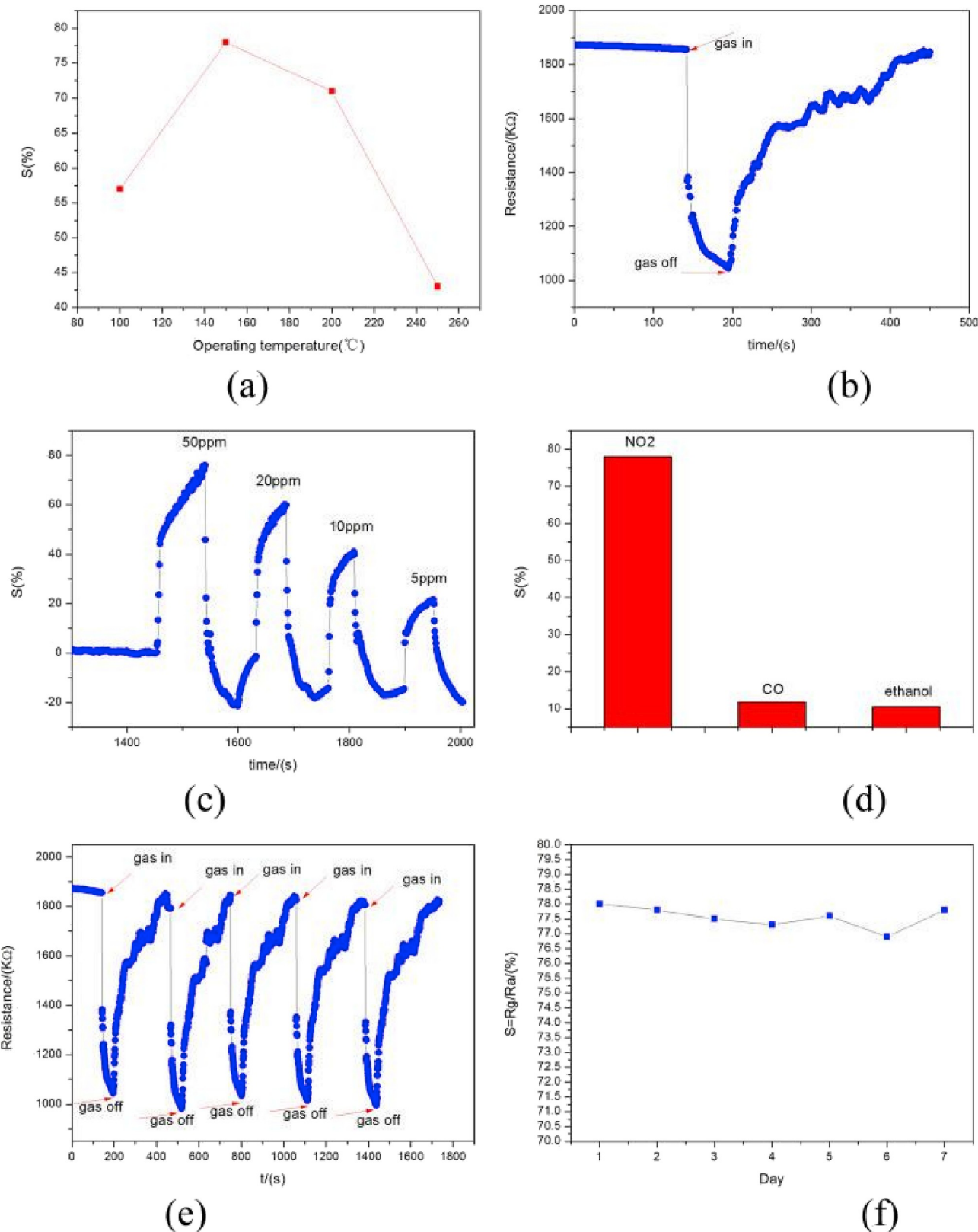


Fig. 3. (a) Temperature dependence study of 3D flower-like MoS_2 spheres, (b) The MoS_2 spheres like 3D flower acts like semiconductor of p-type, (c) Dynamic response for 5–50 ppm NO_2 , (d) The sensitivity and selectivity analysis for various gases, (e) The repeatability analysis of MoS_2 spheres like 3D flower, (f) Stability analysis. Copyright permission from Ref. [15].

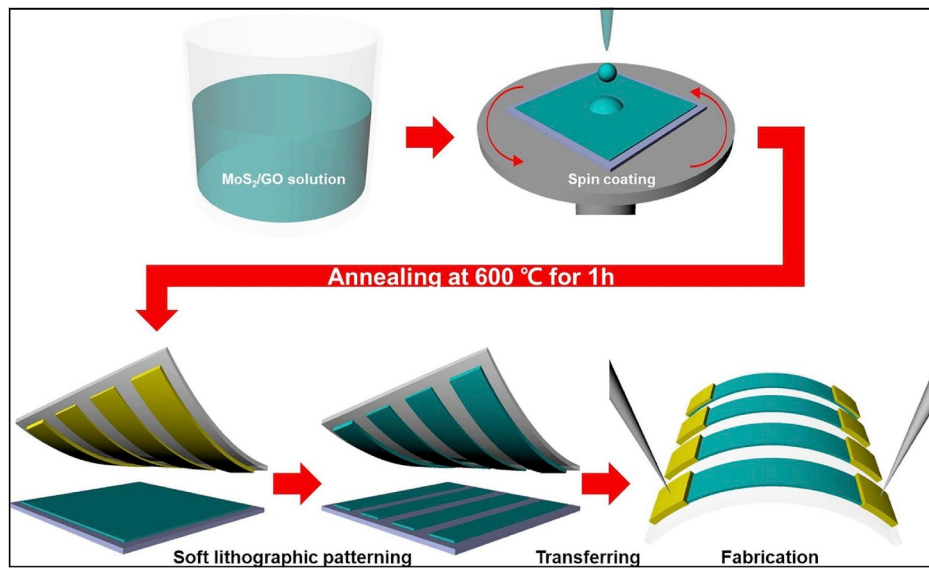


Fig. 4. The complete schematic diagram for the fabrication and patterning of MoS₂/rGO composites. Copyright permission from Ref. [18].

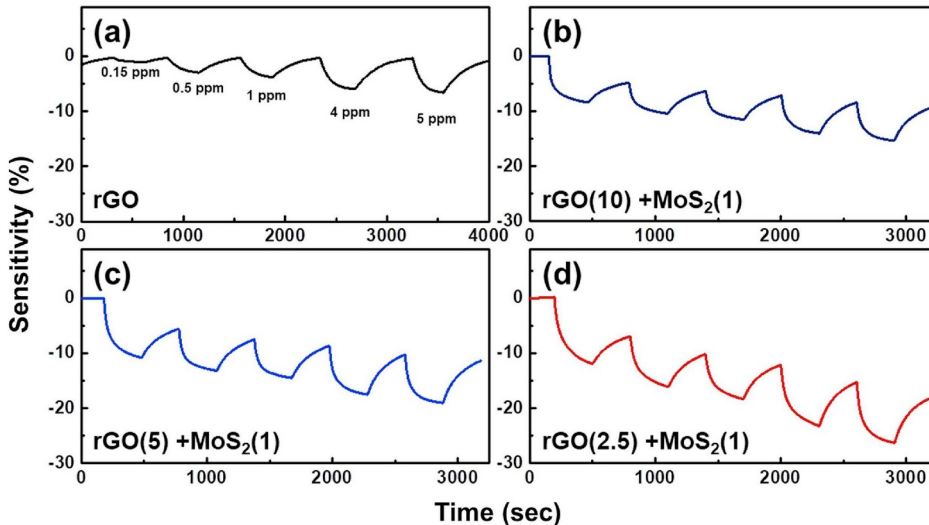


Fig. 5. Variations of characteristics pattern (a) rGO, (b) MoS₂/rGO (1:10), (c) MoS₂/rGO (1:5), (d) MoS₂/rGO (1:2.5) wiry film gas detector with NO₂ gas concentration. Copyright permission from Ref. [18].

influences on the resistance increase, respectively. The p-type response of rGO-MoS₂ is predominantly contributed by rGO. In the presence of 2 ppm of NO₂ gas, the sensing response of the rGO-MoS₂ composite sensor was found at an optimum temperature. In comparison with pure rGO sensor, the response of the composite rGO-MoS₂ sensor is 200% higher as demonstrated in Fig. 7(c and d). In addition to sensitivity, other sensor parameters were also analyzed such as operating temperature, long term stability, humidity effect, selectivity, and detection limit of the rGO-MoS₂ composite sensor. The developed rGO-MoS₂ composite detector was able to detect NO₂ gas with a sensitivity of 59.8% which is 200% higher than pure rGO sensor and also the detection limit of the detector was found as 5.7 ppb.

Sen developed another method for obtaining a high response with fast response and recovery of the sensor by increasing the operating temperature. A two-step wet-chemical method was used for fabricating NO₂ gas sensor by decorating rGO on the surface of MoS₂ NPs [60]. Firstly, a modified liquid exfoliation method was used for preparing MoS₂ NPs from the bulk MoS₂ powder. The self-assembly of MoS₂-NPs and GO sheets were employed for obtaining MoS₂-rGO hybrid sensor,

followed by a hydrothermal treatment process. A certain amount of functional groups still exists in rGO after the synthesis of rGO and MoS₂ using hydrothermal synthesis. Furthermore, some structural defects and vacancies can be introduced during this process, which can also act as adsorption sites for gas molecules. These sites can contribute electrons and holes to the hybrid structure of MoS₂-rGO and hence change the carrier concentration. The p-type rGO and n-type MoS₂ forms a p-n junction resulting in an increase in the sensing performance of the hybrid MoS₂-rGO sensor. The characteristics analysis revealed that the MoS₂ NPs with the size of 3–5 nm are consistently spread over rGO nanosheets. The MoS₂-rGO hybrid sensor was able to detect NO₂ gas even at RT. The typical response curve of the hybrid MoS₂-rGO sensor towards various NO₂ concentrations is shown in Fig. 8(a). The relationship between the NO₂ gas concentrations with the response is demonstrated in Fig. 8(b). The sensing response of the MoS₂-rGO hybrid detector was examined by elevating the operating temperature. It was found that with an increase in operating temperature, the MoS₂-rGO hybrid sensor shows improved response along with fast response and recovery.

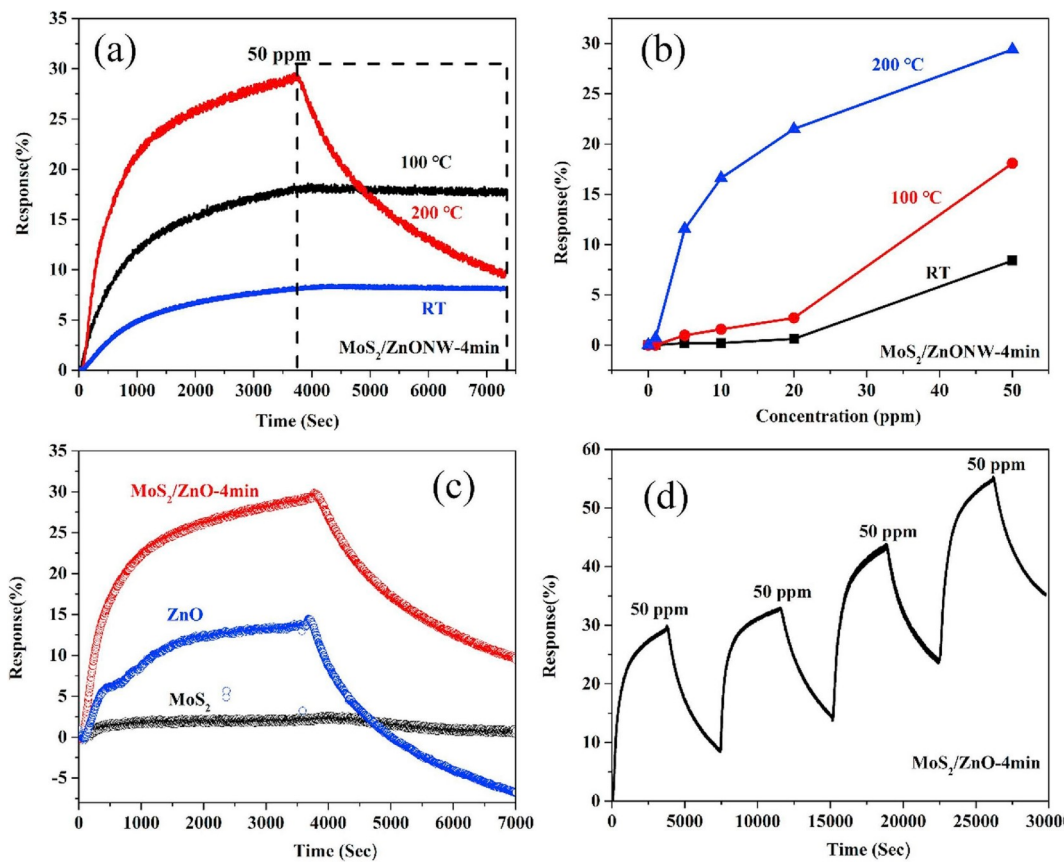


Fig. 6. (a) Dynamic sensing response of MoS₂/ZnO NWs nanostructures for the various temperature to 50 ppm of NO₂. (b) Sensor dynamic response as a function of gas concentration, (c) The sensing response comparison for pure MoS₂, ZnO NWs and MoS₂-ZnO nanowires at 200 °C, (d) The repeatability and response of MoS₂-ZnO nanowires sensor. Copyright permission from Ref. [19].

Recently in 2019, Hairong et al., developed the most efficient method of improving the performance of gas sensing by controlling the surface structure at the atomic scale. Hierarchical MoS₂ microspheres hollow structures were synthesized using a facile hydrothermal approach which offered enhanced NO₂ detection [61]. The active edge sites of MoS₂ were improved by the influx of micro-nano hierarchical design, which favours carrier exchange and increases the kinetics of gas adsorption, eventually resulting in improved sensing behaviour. In comparison to plane solid structure, the hierarchical hollow MoS₂ microspheres with added active sites exhibit outstanding detection capability with 3.1 times improvement. The formation of MoS₂ shell is followed by the nucleation on PS spheres surface facilitated by the polystyrene (PS) templates [see Fig. 9(a)]. The hierarchical morphology is formed as the absorption continues and MoS₂ will nucleate and collect on the nanosheets shell surface [see Fig. 9(b)]. To obtain hierarchical hollow spheres, annealing was done to vaporize the PS spheres template as shown in Fig. 9(c). With increasing the reaction time, shell thickness, roughness of the surface and size of the sphere of spheres also increased. The nucleation of small spheres on the MoS₂ hollow spheres surface occurs and eventually with the reduction in surface energy results in the formation of solid spheres as the reaction time increases to 10 h [see Fig. 9(d)]. The already nucleated small spheres of micrometre size start to grow and eventually separated from the hollow spheres as the time reaches 18 h [see Fig. 9(e)]. The improvement in surface permeability, high surface area promotes gas diffusion, exchange and transportation of the hollow surface area can be associated with the nanosheets comprising the hierarchical micro-nano structure. Consequently, the sensor is capable of working at a lesser temperature with improvement in sensing response. The nanoscale and micro-level surface morphology can be controlled by the introduction of hierarchical structures thereby

rendering new possibilities for improving the detection capability of MoS₂.

The change in the lateral grain size of MoS₂ is also found to improve the sensitivity of the sensor. Junmin et al. developed a high response resistive NO₂ gas sensor by employing a two-step CVD method for growing bilayer MoS₂ [86] [see Fig. 10(a)]. The lateral grain size of the grown bilayer of MoS₂ was 50–100 μm. The response-recovery curve of the as-developed resistive MoS₂ bilayer at RT with varying adsorption of NO₂ is depicted in Fig. 10(b). The response of as-synthesized bilayer MoS₂ resistive gas sensor as a function of NO₂ concentration is depicted in Fig. 10(c). The response of the as-synthesized sensor to 50 ppm of NO₂, CH₄, O₂, NH₃, and H₂ at RT is demonstrated in Fig. 10(d). The as-synthesized bilayer MoS₂ with high lateral grain size is associated with high surface mobility and increased surface evaporation. The developed resistive sensor showed p-type response and reached a super sensitivity at RT. The developed sensor has far better performance in comparison to various previous works [87,88]. The sensing mechanism of the as-developed p-type MoS₂ can be explained as follows. The initial exposure to air of p-type MoS₂ leads to the adsorption of oxygen molecules on the surface, taking away some electrons from the valence band leading to the formation of oxygen species (O₂[−], O[−]). This causes an increase in the hole concentration and a decrease in the resistance. The exposure of oxidizing NO₂ gas to the p-type MoS₂, NO₂ molecules were adsorbed on the surface as NO₂[−] ions, which further extracted electrons from the valence band leading to an increase in hole concentration. The adsorption of NO₂ gas molecules leads to an accumulation of holes, resulting in the formation of the hole layer on the surface of MoS₂. The formation of the hole layer makes the p-type MoS₂ more conductive. When the supply of NO₂ gas is stopped and the p-type MoS₂ is exposed to air again, the adsorbed NO₂[−] species evaporated leaving behind the

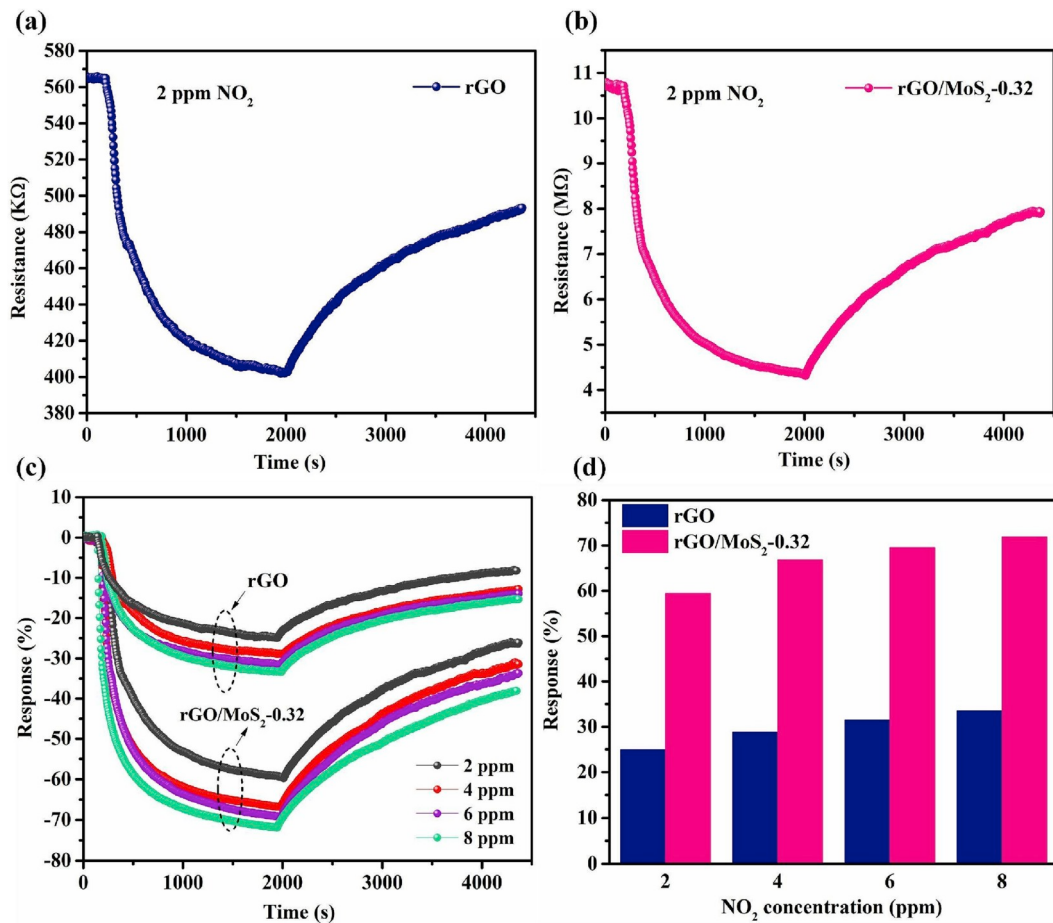


Fig. 7. (a) Dynamic resistance response of rGO sensor towards 2 ppm of NO₂ at 60 °C, (b) Dynamic resistance response of MoS₂ sensor towards 2 ppm of NO₂ at 60 °C, (c) Dynamic detecting response of the rGO-MoS₂ composite sensor, (d) Histogram of the sensing response of both rGO and rGO-MoS₂. Copyright permission from Ref. [58].

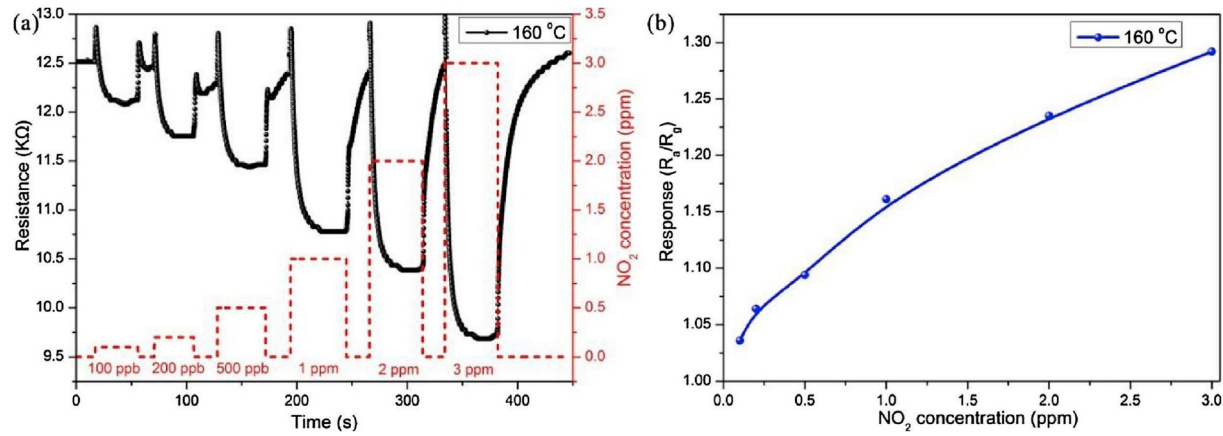


Fig. 8. (a) The typical response curve of the hybrid MoS₂-RGO sensor, (b) The relationship between the NO₂ gas concentrations with the response. Copyright permission from Ref. [60].

captured electrons in p-type MoS₂. The following electron-hole recombination process resulted in a decrease in the hole concentration and an increase in the resistance. At the end of the electron-hole recombination process, the resistance of the p-type MoS₂ returned to the original value. Inversely, when the reducing gases NH₃, H₂, CH₄ are exposed to p-type MoS₂, the electrons chemisorbed by the oxygen species (O₂⁻, O⁻) were released back to the valence band of p-type MoS₂ and combined with holes in the valence band, resulting in the increase of resistance.

Recently in 2019, Shaofeng et al., synthesized an extremely selective NO₂ gas sensor based on a novel rGO-MoS₂-CdS nanocomposite film by facile solvothermal treatment [89]. A new heterostructure is formed where CdS nanocones were grown on the 2D layered rGO-MoS₂ substrate by employing a facile solvothermal treatment. The developed hybrid nanocomposite of rGO-MoS₂-CdS displayed an exquisite selectivity towards NO₂ gas and this can be associated with the structural combination of MoS₂/CdS heterostructure on rGO layer. The detecting

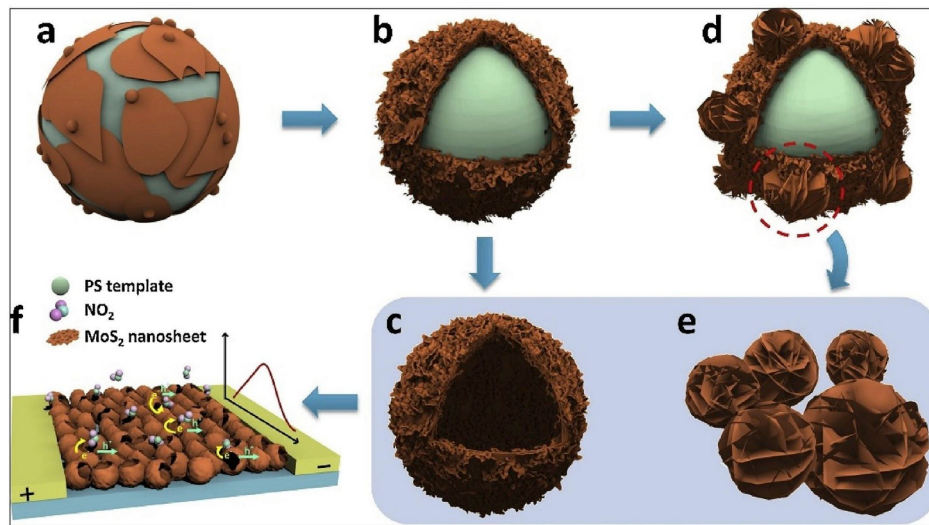


Fig. 9. (a) MoS₂ nanosheets nucleate on the PS template. (b) MoS₂ nanosheets nucleate and develop constantly. (c) The PS spheres template to form the hierarchical hollow spheres, (d) The surface energy reduces because small spheres start to nucleate on the MoS₂ hollow spheres surface and develop into solid spheres, (e) The small spheres grows to micrometre size and separate from the hollow spheres. Copyright permission from Ref. [61].

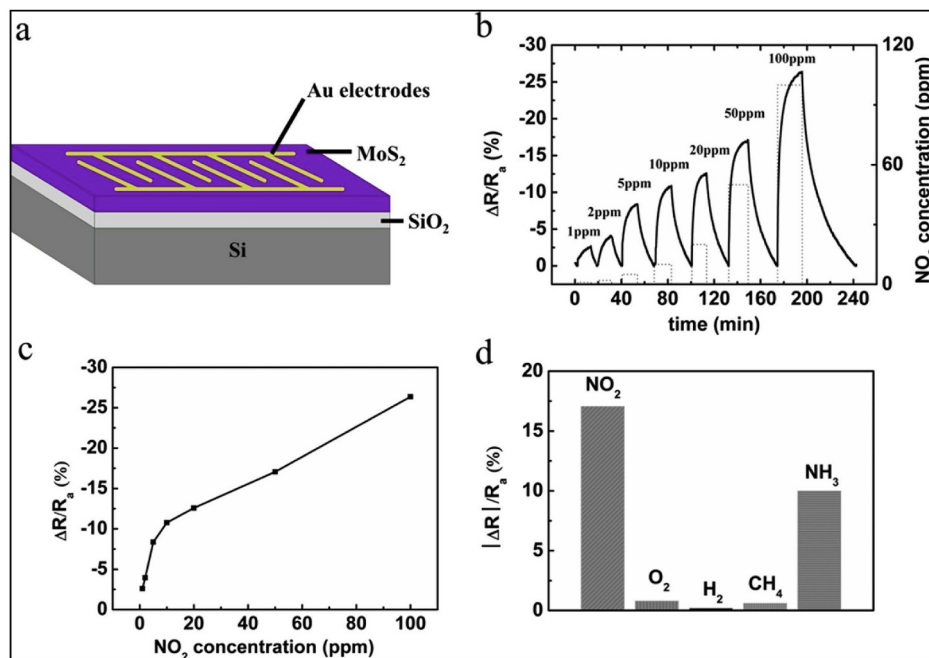


Fig. 10. (a) The schematic diagram of MoS₂ bilayer based resistive gas sensor, (b) The recovery-response curve of the as developed resistance MoS₂ bilayer at various concentrations of NO₂ at RT, (c) The response of as-synthesized bilayer of MoS₂ resistive gas sensor as a function of NO₂ concentration, (d) The response of the as-synthesized sensor to 50 ppm of NO₂, CH₄, O₂, NH₃, H₂ at RT. Copyright permission from Ref. [86].

capability of the synthesized heterostructure rGO-MoS₂-CdS nanocomposite towards numerous concentrations of NO₂ gas has been analyzed. The three different nanocomposites response towards various concentrations, i.e. 0.1–11 ppm of NO₂ is depicted in Fig. 11(b). In all concentration ranges, the repeatability of the sensor was very good. Three different nanocomposite rGO-MoS₂-CdS-a, rGO-MoS₂-CdS-b, rGO-MoS₂-CdS-c sensors with different concentrations of CdS were obtained by solvothermal treatment at 120 °C for 6 h, 12 h and 24 h, respectively. In the solvothermal treatment, increase in time from 6 h to 12 h leads to the homogeneous dispersion of CdS nanocones on the surface of rGO-MoS₂ and hence the formation of more p-n junctions. The sensing response of nanocomposite rGO-MoS₂-CdS-b increased from 10.3% to 25.7% for the same concentrations of NO₂ gas as depicted in

Fig. 11(c). However, the increase in time of solvothermal treatment results in the formation of many hemispheres composed of nanocones and the sensitivity decreases from 25.7% to 16.1%. The nanocomposite sensor before and after NO₂ exposure is depicted in Fig. 11(a). In comparison with other rGO based sensor, the nanocomposite rGO-MoS₂-CdS with lots of heterojunctions, higher specific surface area and more adsorption sites showed an excellent response of 25.7% in the presence of 0.2 ppm of NO₂. Moreover, the hybrid detector depicted an outstanding gas detecting constancy at the operating temperature of 75 °C. This enhanced gas sensing has been explained on the basis of an assumption that O₂⁻ and NO₂⁻ formation takes place on the surface of nanocomposite film. The electron shell depletion region is formed on the surface when nanocomposite film is exposed to air, as surface

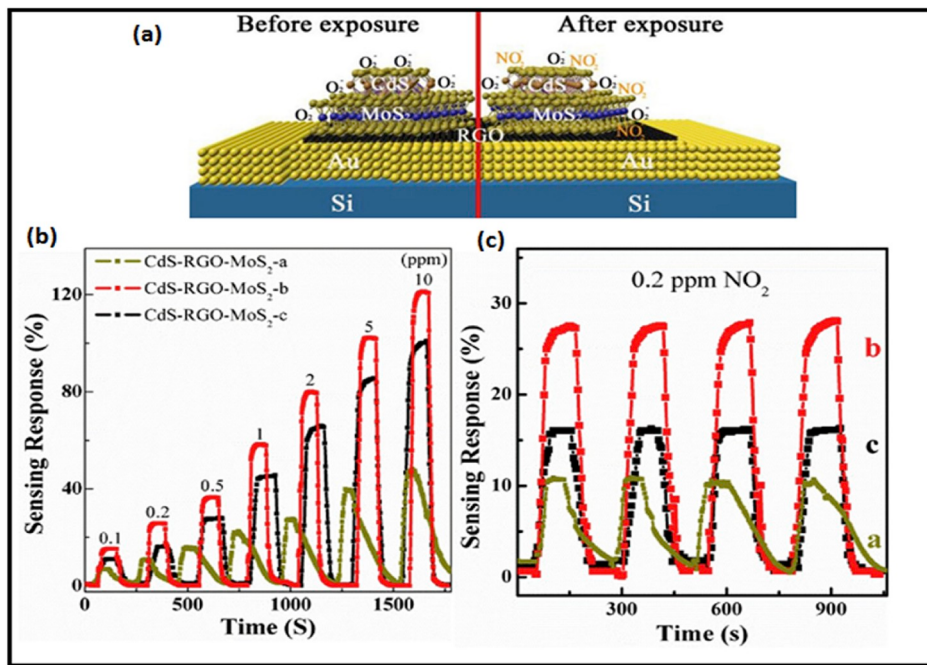


Fig. 11. (a) The nanocomposite sensor before and after NO₂ exposure, (b) The three different nanocomposites response towards various concentrations 0.1–11 ppm of NO₂, (c) The sensing response of the three nanocomposite sensor for same 0.2 ppm of NO₂ gas. Copyright permission from Ref. [89].

adsorbed oxygen will capture electrons from the conduction band of CdS and MoS₂, forming oxygen anions (O₂⁻). This process is responsible for the formation of n-type MoS₂/CdS electron shell depletion region. In the case of rGO, adsorbed oxygen anions cause hole accumulation near the surface of sensing material owing to the electrostatic interaction between opposite charge species. The interaction of NO₂ to rGO is weak and hence NO₂ would be preferentially adsorbed onto the rGO/MoS₂/CdS heterojunctions. The NO₂ molecules adsorption takes place in the form of NO₂⁻, and electrons are continuously withdrawn from rGO/MoS₂/CdS heterojunctions.

In the same year 2019, Zhong et al., employed piezo-phototronic effects and photogating for obtaining single-layer MoS₂ for an enhanced NO₂ gas sensing [90]. The authors irradiated the sensor with a red light-emitting diode (LED) and compared the sensor response in light and dark conditions. The sensor response was also compared by in tensile strain and no strain conditions. In this article [85], an individual layer MoS₂ based NO₂ gas detector with simple and reliable flexibility is presented. The 2D semiconductor characteristics and the ultra-high specific surface area are attributed to the high sensitivity of flexible sensor towards NO₂ gas. The as-developed single-layer MoS₂ sensor showed better performance in terms of sensitivity, recovery and response towards NO₂ as compared to different works done on single-layer MoS₂ [81,91]. The surface charge transfer in the direct bandgap of ultrathin Schottky contacts of MoS₂, photo electricity and also coupling among piezoelectricity can be associated with the sensitivity modulation of the flexible NO₂ sensor.

The enhanced sensitivity and selectivity of the sensor can be achieved by a suitable combination of large active edge sites with a large surface area. Kumar et al. have developed a one-dimensional MoS₂ nanowire network (NW) for enhanced NO₂ gas sensing [92]. The one dimensional MoS₂ NW network was obtained by using controlled turbulent vapor flow from the chemical transport reaction. At different temperatures, the sensing behaviours of the developed MoS₂ NW network were investigated in the presence of discrete molarity of NO₂. The MoS₂ NW network sensor demonstrated 2 fold enhanced sensitivity for NO₂ at 60 °C in comparison with sensitivity at RT and also a very low detection limit. The recovery and response time for the MoS₂ NW network sensor was 172 s and 16 s, respectively at 60 °C while the

sensitivity of the sensor deteriorated at 120 °C. The enhanced sensitivity and selectivity towards NO₂ gas can be associated to a combination of the large surface area along with sufficient active edge sites and calibration of the high voltage barrier at the junction of nanowires during adsorption and desorption of gas molecules. The sensing mechanism of the developed MoS₂ nanowire sensor can be attributed to a change in carrier concentration of MoS₂ owing to chemisorption or physisorption or both, of gaseous molecules. The two factors which are responsible for the variation in the carrier concentrations are the active site density at the surface of MoS₂ and the behaviour (reducing or oxidizing) of gases. At RT both humidity and oxygen occupy a large number of active sites, thereby extracting electrons from the exposed sites of S edge (1010) and Mo edge (10⁻¹0) of the MoS₂ nanowires. Also, due to high vacancy density of the MoS₂ nanowires oxygen is chemisorbed on the sulfur vacancy. This results in a decrease in the concentration of electrons and the creation of the depletion layer. Thus, due to the presence of oxygen and humidity on the surface of MoS₂ nanowires, less number of active sites are available for NO₂ gas molecules adsorption, resulting in a reduction in the response of sensor at RT. Annealing of the device at 60 °C leads to desorption of both humidity and oxygen gas molecules, resulting in the availability of a large number of active sites and electron concentration in MoS₂ nanowires.

Furthermore, Yong et al. developed a unique UV light stimulated room temperature NO₂ gas sensor based on few-layered MoS₂ film decorated with Au nanoparticles [93]. Under dark conditions, MoS₂ sensor in comparison to the as-processed MoS₂-Au depicted a response of 10% in the presence of 2.5 ppm NO₂ which is two times more. The increase in the sensitivity of MoS₂-Au can be attributed to the increase in the reaction sites because of the interfaces and spillover effect and smaller baseline effect due to Au decoration. Incomplete recovery was obtained for all the sensors. The MoS₂-Au based NO₂ sensor under the illumination of UV light depicted three times better response, favourable repeatability and full recovery was accomplished in contrast with the absence of UV light conditions. Two conditions cause the above event. One of the conditions is the effective charge separation at MoS₂-Au interface resulting in repeatable and reversible reactions. The second condition is the additional photo introduced charge carriers which ensure adequate solid-gas interaction between target gas molecules and

sensing layer. The author was able to achieve room temperature, UV light assisted, sensitive, reversible and highly selective NO₂ gas sensing based on a few layers of MoS₂-Au nanocomposites serving as sensing layer.

The major challenge regarding sensors based on MoS₂ is that the sensor suffers from long recovery and response time, specifically at room temperature. Kumar et al. developed the photo-activated extremely reversible and quick sensing of NO₂ at RT by employing improved p-MoS₂ flakes with blend in edge and plane [94]. The detector depicted a fast response with a sensitivity of about 10.6% for 10 ppm NO₂ without complete recovery. However, full recovery was achieved by UV light illumination at RT. The UV aided NO₂ sensing showed enhanced sensing in terms of fast recovery and response with increased sensitivity towards 10 ppm NO₂ at room temperature.

In the year 2018, Yang et al. fabricated a hetero-nanostructure of MoS₂/ZnO for enhanced NO₂ gas detection at room temperature (RT) [95]. Hetero-structure fabrication is an impressive approach to alter the electronic behaviour of intrinsic MoS₂ nanosheets, thereby accomplishing high sensitivity and outstanding recovery properties. A simple wet chemical method was employed to fabricate a novel p-n hetero-nanostructure on MoS₂ nanosheets using surface modification. The surface modification of MoS₂ with nanoparticles of zinc oxide (ZnO NPs) results in the formation of hetero-nanostructure of MoS₂/ZnO which is capable of outstanding performance of 3050% to 5 ppm NO₂, which is eleven fold more than that for pure MoS₂ NPs sensor. The hetero-nanostructures of MoS₂/ZnO exhibit p-type characteristics, which shows that the major charge carriers are MoS₂ NSs and ZnO NPs act as active decorations. In case of pristine p-type MoS₂ NSs, the defects on the surface of MoS₂ act as active sites for NO₂ gas molecules. The response and recovery are slow due to the defect dominated process owing to high adsorption energy. During the sensing process, the electrophilic NO₂ molecules capture electrons from the conduction band of MoS₂, leading to an increase in the conductivity of the sensor. The as-developed hetero-nanostructure is capable of more than 90% recovery at RT. Also, the sensor possesses a very fast response time of the 40 s, great stability, outstanding selectivity and lower detection limit of 50 ppb. The as-developed MoS₂/ZnO hetero-nanostructure showed better performance in comparison with many previously reported articles [15,20,96].

In the same year, Kumar et al. employed a controlled vapor transport process for obtaining hybrid microflower of MoS₂-MoO₃ for an efficient gas sensing at RT [97]. Various characterization techniques were used for studying crystal structure and morphology of the developed hybrid micro flower. The hybrid micro flower analysis with a cathodoluminescence mapping revealed that the flower petals, as well as nanosheets, are composed of MoS₂ while the core of micro flower comprises of MoO₃. Without any external stimulus (like thermal or optical), the hybrid MoS₂-MoO₃ sensor exhibited a sensitivity of 33.6% towards 10 ppm NO₂ gas with complete recovery at RT. In comparison with various earlier reports on MoS₂, the as-developed MoS₂-MoO₃ sensor showed a low response time of 19 s with total recovery and an outstanding selectivity towards NO₂ against different other gases at room temperature. The sensing mechanism is associated with a build-up of modulation of a potential barrier at the interface of MoS₂-MoO₃ during desorption/adsorption of NO₂ and high hole injection from MoO₃ to MoS₂. Also, this article demonstrates that by controlling the micro and nanostructures the properties of 2D materials can be altered toward utilization in modern electronics. Energy band diagram is used to explain the sensing mechanism of MoS₂-MoO₃ hybrid. The work function of MoO₃ and MoS₂ are 5.3 and 4.7 eV, respectively. This energy offset band of 0.6 eV forms a potential barrier and leads to efficient electron-hole separation at the n-MoS₂/n-MoO₃ junction. The potential barrier at the n-n heterojunction plays an important role in the modulation of the conduction channel width that is essentially responsible for the fluctuation of the device resistance.

It was found that at room temperature, in comparison to horizontally

aligned MoS₂ flakes, the vertically aligned (VA) MoS₂ flakes exhibited two times higher response to NO₂. Kumar et al., developed the VA-MoS₂ flakes network-based highly sensitive and reversible NO₂ resistive gas sensor [98]. A kinetically restrained fast growth approach of CVD process was used for synthesizing vertically and horizontally aligned MoS₂ flakes on SiO₂/Si substrate. At an optimized operating temperature (100 °C), the detector depicted complete recovery upon NO₂ exposure. The sensing behaviour of VA-MoS₂ sensor was studied for various gases such as CO₂, H₂S, NH₃, CH₄ and H₂. The VA-MoS₂ sensor exhibited great selectivity towards NO₂ gas with a high response as well as good reversibility. These responses can be associated with the large aspect ratio, high adsorption energy on exposed edge sites, strong interaction between gas molecules and the exposed edge sites at the interface.

2.1.2. Miscellaneous TMDs based NO₂ gas sensors

Tingting et al. introduced a new material for NO₂ gas sensing, i.e. WS₂ nanosheets. The developed resistive gas sensor based on WS₂ demonstrated a p-type behaviour and the sensor was able to achieve a superior response of about 9.3% for 0.1 ppm NO₂ at room temperature. The detector showed superb stability in low and moderate humidity. The increase in the sensitivity of WS₂ gas sensor towards NO₂ gas can be attributed to the rough surface and ultrathin nanostructure of WS₂ nanosheets. Hydrothermal and calcination processes were employed for developing ultra-thin WS₂ nanosheets for ultra-high sensing response of NO₂ gas [59]. A thickness of about 5 nm of ultra-thin WS₂ nanosheets was achieved by employing cost-effective hydrothermal approach followed by calcination technique. The interconnection of WS₂ nanosheets led to the formation of a three-dimensional wall like the design. The typical response-recovery characteristics demonstrated that in the presence of NO₂, the resistance decreases rapidly, and the response of the gas detector elevated with NO₂ concentration as depicted in Fig. 12(a). With varying the concentration of NO₂, the corresponding responses also changed significantly. The relationship between the gas sensing response and concentration of NO₂ gas is depicted in Fig. 12(b). The repeatability of the gas sensor towards 5 ppm NO₂ gas is demonstrated in Fig. 12(c). The response of WS₂ sensor in this work is better as compared to the previous works [86,99]. The cycling response for 5 ppm NO₂ shows no decline in sensor response for five cycles, thus, substantiating good repeatability of WS₂ detector.

In the year 2018, Roya et al. proposed unique structures of WS₂/graphene aerogel hybrid to enhance the selectivity of NO₂ gas detection. They investigated the influence of temperature and ambient humidity on the NO₂ detecting tendency of WS₂/graphene sensor [16]. Two electrodes were microfabricated on the surface of WS₂/graphene hybrid aerogel in order to probe its gas detecting performance. The characterization of hybrid WS₂/graphene aerogel composite establishes the existence of both graphene and WS₂. The continuous 3D nanostructure material deposited on sensor material is established. Also, it has been confirmed that in hybrid aerogel composite, WS₂ and graphene are distinguished by lattice spacing indicating WS₂ is one to five-layered and graphene being one to six-layered. At room temperature, with an increase in humidity, sensing response and recovery towards NO₂ gas also increase. In a dry atmosphere, with an increase in temperature till 180 °C, recovery and response rates also increase and signal recovery is enhanced, however, signal feedback is decreased. The hybrid WS₂/graphene aerogel composite sensor showed excellent selectivity towards NO₂.

Alexander et al. fabricated gold decorated WS₂ nanotube photoresistive sensor for NO₂ gas detection [100]. An aqueous solution of HAuCl₄ was used to prepare a composite of gold nanoparticles (AuNPs) and WS₂ nanotubes. Plasmonic features of the obtained nanocomposites were confirmed with the help of electron energy loss spectroscopy in scanning transmission electron microscopy regime (STEM-EELS) and Optical extinction spectroscopy. It was found that at room temperature the NT-WS₂ and Au-NT-WS₂ depicted a remarkable sensitivity towards NO₂ under illumination from 530 nm light-emitting diode. In the range

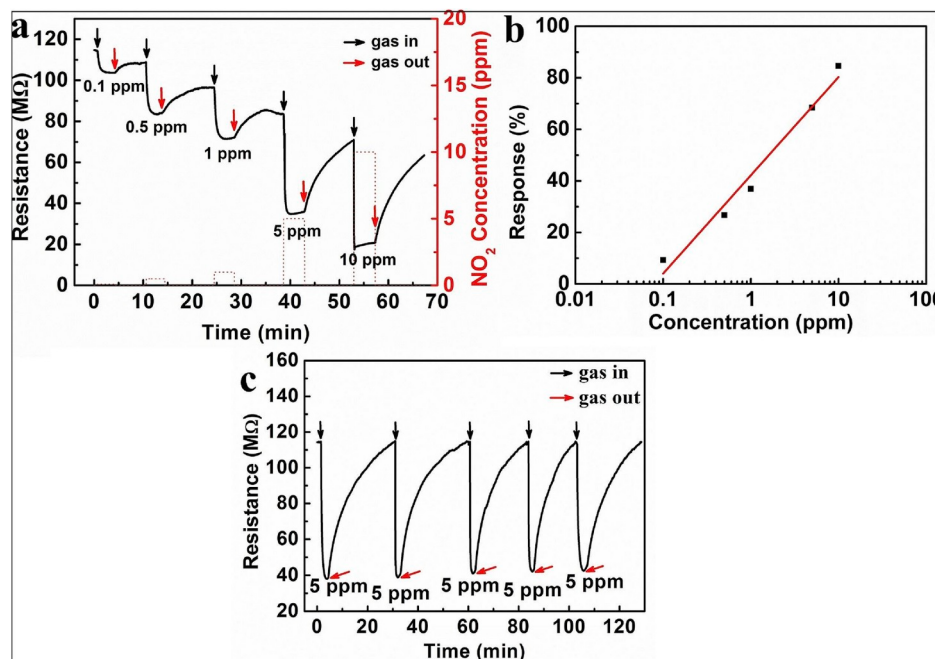


Fig. 12. (a) The typical response-recovery curve with various concentration of NO₂, (b) The relation between response and concentration of NO₂, (c) The repeatability of the WS₂ gas sensor in the presence of 5 ppm of NO₂. Copyright permission from Ref. [59].

of 0.25–2.0 ppm of NO₂, the Au-NT-WS₂ nanocomposites sensor exhibited an enhanced sensitivity and higher photo-response as compared to pristine NT-WS₂.

Yongxiang et al. developed SnS₂ based wireless gas sensor which demonstrates extreme selectivity towards NO₂ gas. For fabricating sensor, they used a low temperature co-fired ceramic technique (LTCC) and a resonant antenna circuit [101]. The sensor structure designed as LC were both IDC (C_s) and a planar square spiral inductor (L_s) integrated on LTCC structure. A resonant circuit was obtained by connecting both capacitor and inductor into LTCC body. In order to determine the resistance of the LC sensor through physisorption-based charge transfer and polarization effect after NO₂ adsorption, a sensitive film of 2D SnS₂ was laminated on the IDC electrodes. The highly selective and sensitive behaviour of 2D material SnS₂ towards NO₂ gas makes it a suitable material for sensing film. A comprehensive analysis of the developed wireless sensing mechanism was done for NO₂ gas. The variation in the resistance and dielectric properties of the sensing film is attributed to the physisorption based interaction between 2D SnS₂ surface and NO₂ gas, influencing the physical response of the LC antenna sensor which is in complete agreement with previous work [102]. Investigations under the influence of various concentrations of NO₂ at different temperatures found the wireless gas sensor to exhibit the highest response at 120 °C with a low detection limit of 0.6 ppm. In the wireless gas sensing and analysis, the developed sensor could be very useful as it has good response and response profiles. Moreover, this work also demonstrated the feasibility of integrating various other sensitive materials on LTCC platform for various gas species.

Khan et al. developed an extremely selective and ultra-sensitive NO₂ gas detector employing quasi physisorption 2D tungsten oxide (WO₃) [103]. The first step of the analysis was to find out an optimum temperature which gives a maximum response with fast response and recovery. It was found that the rise in temperature boosted the sensor response but recovery and response times decreased. The optimum temperature for the developed sensor was found to be 150 °C as with the further increase in temperature the response decreases. The reason for this behaviour can be interpreted by the fact that at higher temperatures, the rate of adsorption becomes less than the rate of desorption and consequently the response decreases [104]. Two samples heated at

450 °C and 225 °C give a response factor of ~4 and ~15, respectively at 20 ppb of NO₂ gas concentration. The reversibility of both sensors was excellent as both sensors recovered their baselines fully. However, recovery of the sensor heated at 225 °C was faster in comparison to the sensor heated at 450 °C. The NO₂ gas molecules adsorbed on surface act as an electron acceptor and accept electrons from WO₃ [102]. Owing to the charge transfer mechanism, the number of free electrons is reduced and the resistance increases, which is the n-type behaviour. The increase in sensitivity of the sensor annealed at 225 °C can be accredited to the better synergy between NO₂ gas molecules and stronger dipole material WO₃. The semiconducting nature of 2D sheets of WO₃ annealed at 225 °C have been established by XPS analysis. However, the sample annealed at 450 °C and the unannealed sample showed metallic behaviour and hence require more electrons for full-on/off switching. The other reason in case of unannealed is sample hydration while in case of the sample heated at 450 °C is not a fully monoclinic structure of the sample. In the case of the sample heated at 225 °C, a combination of semiconducting nature, hydration, degraded oxygen vacancies and monoclinic crystal structure is responsible for higher selectivity and sensitivity towards NO₂ gas.

The 2D transition metal dichalcogenides (TMDs) based sensor performance for sensing NO₂ gas has been discussed. These sensors are more durable and convenient in terms of methods of preparation, structure, materials used, the concentration of NO₂ gas, response and recovery times, and operating temperature. Numerous samples and progress in the development of NO₂ based gas sensors using TMD nanostructures and its hybrid have been enumerated in Table 1.

2.2. Metal-oxide based nanostructures

A detailed research on sensing applications based on metal oxides have shown that the sensing phenomenon is very complicated and it depends on many parameters of metal oxides such as thickness, porosity, grain size, catalytic reactivity, grain network, agglomerations, bulk conductivity, surface stoichiometry, surface architecture, bandgap and so on [14,105–108]. Analysis of gas sensors based on metal oxides has shown that there is a great influence of above-mentioned factors on gas sensing behaviour of the developed sensors. With respect to the

above-mentioned parameters, the optimization of gas sensors has been achieved by applying many technological approaches [109]. It has been shown that all the important properties of metal oxides for gas sensing applications can be really influenced by the control of the deposition parameters, doping during synthesis or deposition and post-deposition treatments.

2.2.1. ZnO nanowire based NO_2 gas sensors

ZnO has may shape and structural forms under various growth conditions. Wurtzite is thermodynamically the most favoured form of ZnO under ambient conditions. Oxides of Zinc, Tin, Titanium, etc., are usually used in metal oxide-based semiconductor sensors as sensing element. Moreover, nanostructured metal oxides are promising candidates as a gas sensor due to their large surface-to-volume ratio which is more desirable for the diffusion of target gases in sensor material.

A highly selective NO_2 gas sensor with fast response and recovery and high sensitivity was developed using ZnO nanowires (ZNW) array [110]. A seed layer deposition technique was used for preparing arrays of ZNW on the surface of the detection electrode. A facile hydrothermal route was followed by Shen et al. for developing arrays of ZNW in-situ grown on detecting electrode for NO_2 gas detection [110]. In seed growth system, a $\text{Zn}(\text{CH}_3\text{COO})_2 \cdot 2\text{H}_2\text{O}$ ethanol solution was used with $\text{Zn}(\text{NO}_3)_2 \cdot 6\text{H}_2\text{O}$ -HMTA ($\text{C}_6\text{H}_{12}\text{N}_4$) as a hydrothermal route in a dipping process. The gas detecting response of the ZNW arrays revealed that the detector had good selectivity and reproducibility, as well as the response of the sensor, showed a linear dependence on NO_2 concentration in 1–30 ppm range. The ZNW array sensor was highly selective to NO_2 with fast recovery time, fast response and high sensitivity. At the optimum temperature of 200 °C, the ZNW array sensor showed a maximum response towards 3.3–5 ppm of NO_2 gas with fast recovery and response times of 21 s and 25 s, respectively. The developed ZNW array by facile hydrothermal route is favourable for commercial applications. The electron depletion theory is used for explaining the sensing mechanism of ZNW arrays to NO_2 . The oxygen molecules are adsorbed on the surface of ZNW arrays when exposed to air. These oxygen molecules then capture electrons from the conduction band of ZNW and transform into ionic species (O^{2-} , O^- , O_2^-). This electron transfer forms an electron depletion region on the surface of ZNW arrays. Hence the resistance of the ZNW arrays is increased as major charge carriers in n-type ZnO semiconductor are electrons. When NO_2 molecules adsorb on ZnO nanowires surface, they continuously capture electrons from the conduction band. This is because the electron affinity of the NO_2 gas is higher than oxygen. In this way, the concentration of electrons in the conduction band decreases drastically, resulting in the larger electron depletion region and higher resistance. Upon NO_2 desorption, the resistance of ZNW arrays returns to its initial value.

In the following year 2018, Cui et al. developed a unique and path-breaking technique to reduce the operating temperature of metal oxide-based NO_2 gas sensors [111]. A three-step facile process was used for preparing two different structures, i.e., ZnO–CuO NWs (ZnO nanowires decorated with CuO nanoparticles) and nanowires of ZnO–CuO core-shell (C-S NWs). The response for both reducing gas benzene and oxidizing gas NO_2 were analyzed. Heterostructures of ZnO–CuO were obtained by a thermal oxidation process from heterostructure of ZnO–Cu C-S NWs in the temperature ranges from 300 to 600 °C for 1 h. The heterostructures of ZnO–CuO were investigated by FESEM in the presence of various oxidizing conditions. The top layer is the ZnO–CuO heterostructures; the middle layer is the ITO film, and the bottom layer is the glass substrate. Thermal oxidation at a relatively low temperature of around 300 and 400 °C maintains the C-S structures of NWs while thermal oxidation at higher temperatures of around 500 and 600 °C reduces the roughness of the sample which is mainly attributed to the increase in the crystallinity of CuO at higher temperatures. At higher temperatures (500 °C & 600 °C), the C-S composition changed to nanoparticles named as ZnO–CuO NWs. The optimum operating temperature in the presence of benzene for ZnO–CuO C-S NWs was 250 °C

while for an oxidizing gas like NO_2 , it was around 300 °C for ZnO–CuO NWs and 350 °C for ZnO NWs. The p-type response of ZnO–CuO NWs indicates that ZnO NWs influence carrier transportation within the sensing layer. On the other hand, ZnO–CuO C-S NWs demonstrate n-type behaviour indicating the dominance of CuO shell in sensing performance. In conclusion, it was found that ZnO–CuO NWs and pure ZnO NWs show increased sensing performance while ZnO–CuO C-S NWs exhibit poor sensing behaviour.

For increasing the response of NO_2 sensor at low operating temperature, Shen et al. proposed Pd doping in ZNWs. They observed that the response of sensor increased with increment in Pd doping. They made Pd-functionalized ZnO nanowires (Pd-ZNWs) by exploiting a facile hydrothermal one-pot approach [28]. Post hydrothermal process, the Pd was self-configured on ZnO nanowires surface (ZNWs). The characteristics analysis of the developed Pd-ZNWs demonstrates that the Pd functionalization has not influenced the morphology and size of ZNWs. In comparison to pure ZNWs, the functionalized Pd-ZNWs sample showed lower operating temperature, higher response, faster recovery and response towards NO_2 . A combination of chemical and electronic sensitization of Pd is responsible for the sensing mechanism of Pd-ZNWs. The dissociation of NO_2 into ionized or nonionized species such as NO , NO^+ and O on the surface of ZNWs can be facilitated by the chemical sensitization of Pd/PdO nanoparticles. The dissociated species are transferred on the surface of ZNWs by means of a spillover effect. Hence, the electrons from the conduction band of ZNWs can be readily captured by the dissociated species, resulting in wider electron depletion layer and large resistance variation.

Lingmin et al. developed a 3D hybrid optoelectronic NO_2 gas sensor with enhanced sensing capabilities in 2018 [112]. In this work, the facile solution method, thermal reduction and spray deposition techniques were employed for obtaining ZnO nanowalls grown in-situ on the surface of porous rGO (PG). The result showed that 3D ZnO-PG hybrid nanocomposites composed homogeneously interconnected 3D ZnO nanowalls network on the surface of PG films. The developed 3D hybrid is responsible for providing channels for gas diffusion. The ZnO-PG hybrid nanocomposite sensor exhibited good photodetecting response of 7.4 under 365 nm UV irradiation. The sensitivity of the sensor towards 50 ppm NO_2 was found to be 35.31 at RT under the UV illumination of 1.2 mW/cm². In comparison with pure ZnO sensor, the sensitivity of 3D ZnO-PG hybrid sensor was 2.24 folds higher [113,114]. For 50 ppm of NO_2 , the recovery and response times for the hybrid sensor were ~2 s and ~37 s, respectively. In the ambient atmosphere, oxygen molecules adsorb on the surface of ZnO nanowalls and ionize to O_2^- by capturing free electrons from the surface of ZnO to generate a high depletion region with high resistance at the surface. The energy bandgap of ZnO is 3.2 eV which is lower than photo energy of UV irradiation (3.4 eV). Electron-hole pairs are photo-generated when UV light is irradiated on ZnO nanowalls, followed by migration of holes to the surface and the O_2^- species are photo-desorbed. As a result, the remaining unpaired electrons will contribute to the decrease in electrical resistance and the depletion layer is diminished. In the presence of NO_2 gas, the adsorbed NO_2 gas molecules capture the photo-generated electrons and react with adsorbed oxygen ions thereby, increasing the resistance of the sensing material. In the case of hybrid structure, the Fermi energy level of ZnO is lower than rGO owing to the difference in work functions of n-ZnO (5.20 eV) and PG (4.75 eV). This facilitates the charge transfer from PG to the conduction band of ZnO and further increases the adsorption of NO_2 .

In the same year, Nguyen et al. proposed another technique for developing metal oxide-based gas sensor [115]. Thermal evaporation process was used for on-chip growth of Zn_2SnO_4 and ZNW. In this report, the effects of distance between the microelectronic chip and the source on the gas on sensing behaviour of the developed sensors Zn_2SnO_4 and ZNW were investigated. It was found that the alignment of microelectrode chips of 2–6 cm size results in the identical consequence for ZnO nanowire detectors but an order of degree change in response for

Zn_2SnO_4 as deliberated at 10 ppm of NO_2 gas. The response of Zn_2SnO_4 nanowire sensor towards 10 ppm of NO_2 in comparison with ZNW sensor is significantly higher. The comparative gas sensing studies of both Zn_2SnO_4 and ZNW sensors revealed that the former exhibits better sensitivity and selectivity towards NO_2 gas. With an increase in the growth time duration of Zn_2SnO_4 , the sensitivity towards NO_2 gas increases. However, the sensitivity decreases if the growth time is prolonged beyond. The sensing mechanism can be explained on the basis of reaction of reduced gases with adsorbed oxygen on the surface of NWs.

In the following year, Yanbai et al. demonstrated a unique technique for obtaining better selectivity towards NO_2 gas as well as the sensing response approaching the theory of power laws. They used a hybrid structure of ZNW and Au nanoparticles for enhancing the sensing of NO_2 gas [116]. A facile one-pot hydrothermal approach was used for the synthesis of ZNWs with various concentrations of Au nanoparticles to obtain hybrid Au-ZNWs and ZNWs. The structural analysis of Au-ZNWs revealed that Au nanoparticles self-assembled on the surface of ZNWs and addition of HAuCl_4 have suppressed the c-axis growth of ZNWs in the synthesis of Au-ZNWs. The gas detecting performance of the hybrid sensor was analyzed and it was found that in comparison with pure ZNWs sensors, the Au-ZNWs sensors showed better sensitivities [117, 118]. The maximum response for 1 mol% Au-ZNWs hybrid sensor at 150 °C was 31.4 which is 4 times higher in comparison with the pure ZNWs sensor response of 8.2. Also, it was found that 1 mol% Au-ZNWs hybrid sensor has the shortest recovery and response time of 18 s and 29 s for an extended spectrum of performing temperature. A hybrid sensor of Au-ZNWs sensor with various concentrations of Au has shown better selectivity towards NO_2 gas in comparison to pure ZNWs sensors. The relationship between the concentration of Au in the hybrid Au-ZNWs sensor and the sensing response follows the theory of power laws. The modulation of the electron depletion layer is responsible for the NO_2 gas sensing mechanism of pure ZNWs. In the ambient air, oxygen molecules will be adsorbed on the surface of ZNWs by trapping the free electrons in the conduction band of ZnO semiconductor. This results in the formation of an electron depletion region. In the presence of strong oxidizing gas, e.g. NO_2 , NO_2 gas molecules adsorb on the surface of ZnO and O_2 gas molecules are removed from the surface with the

release of free electrons. In comparison to oxygen, NO_2 gas molecules have higher electron affinity. Therefore, the NO_2 gas molecules will trap more electrons and convert to NO_2^- , thereby facilitating the formation of a larger electron depletion region with higher resistance. Self-assembly of Au nanoparticles on the surface of ZNWs creates more active sites for NO_2 molecules adsorption, which is known as a spillover effect. Besides, Au nanoparticles also facilitate the dissociation of NO_2 gas molecules into ionized or neutral species, possibly including O , NO , NO^+ . These disassociated species are transported to the surface of ZNWs by spillover effect, which is the main reason for faster recovery and response after Au functionalization.

Another group led by Tai et al., in 2017 developed a light aided NO_2 gas sensor based on $\text{ZnO}-\text{Ag}$ nanoparticles for enhanced gas sensing response at room temperature [120]. A modified polymer structure gel technique was used for preparing hybrid $\text{ZnO}-\text{Ag}$ nanoparticles. They observed an enhancement in surface oxygen vacancies, which was attributed to the formation of heterojunction between the two materials. In comparison with pure ZnO , the sensitivity of $\text{ZnO}-\text{Ag}$ to NO_2 gas (0.5–5 ppm) is increased under the influence of different irradiations ($\lambda = 365$ –520 nm). The room temperature resistive response under the illumination of 430 nm light of $\text{ZnO}-\text{Ag}$ heterostructured nanoparticles to NO_2 gas from 0.5 to 5 ppm is displayed in Fig. 13(a). Similarly, the response curve for the $\text{ZnO}-\text{Ag}$ hybrid structures is displayed in Fig. 13(b). Fig. 13(c) demonstrates the responses of ZnO and $\text{ZnO}-\text{Ag}$ nanoparticles for the concentration variation from 500 ppb to 5 ppm under the influence of 430 nm of light at RT. The various sensor responses to NO_2 under the influence of various wavelengths of light is described in Fig. 13(d). These analyses revealed an excellent heterojunction between AG-NPs and ZnO particles. The enhanced gas sensing is mainly because of the synergism developed due to the Ag deposition and oxygen vacancies. The SPR effect of Ag-NPs produced on the surface of ZnO under the influence of UV illumination holds great potential for $\text{ZnO}-\text{Ag}$ nanoparticles as an application for gas detection. Enhancement of charge separation is mainly done due to the formation of electron sink of surface oxygen vacancies and AgNPs. The positive impacts of moisture on the sensing performance of NO_2 of the as-developed heterostructures can be associated with the photocatalytic reception associated with

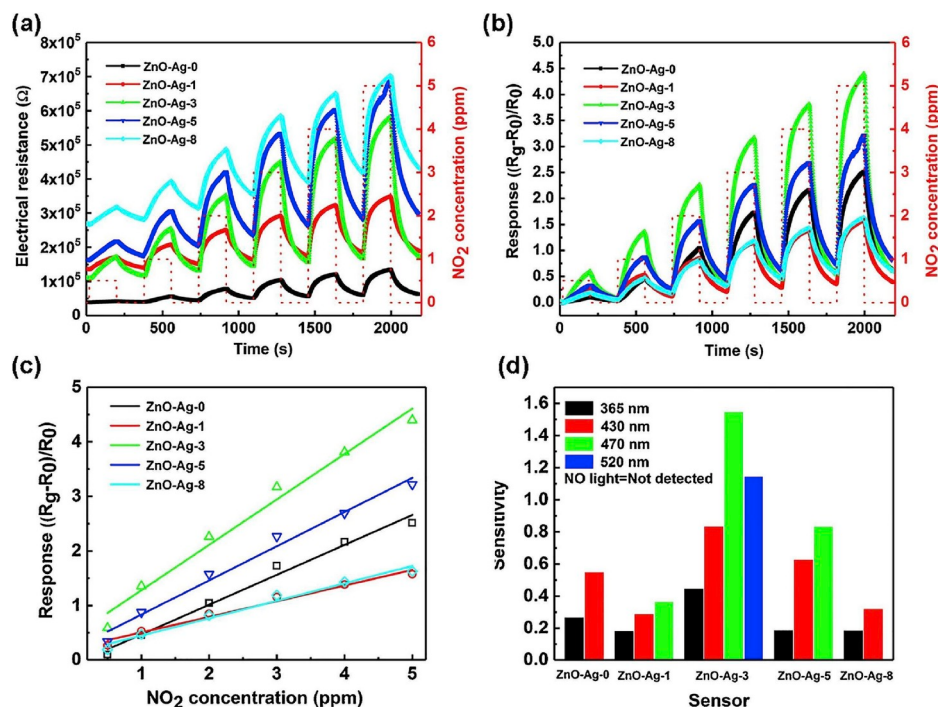


Fig. 13. (a) Resistance plots, (b) Response plots, (c) Response curves for $\text{ZnO}-\text{Ag}$ in the range of 500 ppb to 5 ppm under the illumination of 430 nm light at RT, (d) The sensitivities of various sensors to NO_2 gas under the illumination of various wavelengths of light. Copyright permission from Ref. [120].

water molecules.

Chongmu et al. also developed a highly sensitive gas sensor by adopting a unique method of increasing the surface area. A composite structure of Pd-ZnO co-decorated SnO₂ nanorod sensor was fabricated for enhanced NO₂ gas sensing performance [130]. A three-step process was used for synthesizing SnO₂ nanorod co-decorated with Pd-ZnO: the thermal evaporation of Sn powder was used for SnO₂ nanorod synthesis persuaded by a sol-gel accumulation of Pd and ZnO NPs. The response of the developed nanorod sensor is examined in the presence of NO₂ gas. The Pd and ZnO NPs were composed of face centred cubic structured Pd single crystal and wurtzite-structured ZnO single crystal, while the nanorods comprised primitive tetragonal structured single-crystal SnO₂. TEM and corresponding electron diffraction of co-decorated ZnO-Pd on SnO₂ surface are shown in Fig. 14(a-d). The temperature dependence of the sensor response in the case of both pristine SnO₂ and Pd-ZnO-SnO₂ is shown in Fig. 14(e). The dynamic sensing response of different detectors for NO₂ gas at 300 °C is shown in Fig. 15(a-d). The comparison of dynamic sensing response of pristine SnO₂ nanorods, the response of ZnO decorated SnO₂, Pd decorated SnO₂ nanorods and Pd-ZnO co-decorated SnO₂ nanorod is shown in Fig. 15(a-d). It was found that in comparison with ZnO or Pd decorated SnO₂ nanorods, the Pd/ZnO co-decorated SnO₂ nanorods showed a remarkably improved sensing response towards NO₂ gas. Also, Pd-ZnO co-decorated sensor has a fast response and higher selectivity in comparison to pristine sensors. The SEM morphology analysis displayed that both ZnO and Pd touched each other in Pd-ZnO co-decorated SnO₂ nanorods. The main reason for the difference in the sensing response between pristine and co-decorated SnO₂ sensor is the formation of ZnO-SnO₂ and Pd-SnO₂ interface. The gas sensing mechanism of the Pd/ZnO co-decorated SnO₂ nanorod is based on ZnO-SnO₂ and Pd-SnO₂ interface. Electrons transfer from SnO₂ to ZnO in a vacuum after contact, owing to higher fermi level of SnO₂ than that of ZnO resulting in the formation of accumulation and depletion on the SnO₂ and ZnO sides, respectively near the ZnO-SnO₂ interface. In ambient air, the adsorbed oxygen molecules capture electrons from the conduction band of SnO₂ and ZnO and transform into oxygen ions, depending on the operating temperature. This results in the formation of the depletion layer on both SnO₂ and ZnO sides of ZnO-SnO₂ interface. In addition to the formation of a depletion layer, a potential barrier with a height of E₁ is also formed at the interface. In the presence of NO₂ gas molecules, more transfer of electrons from the conduction band of SnO₂ and ZnO to the adsorbed oxygen takes place, leading to the formation of wider depletion layer on both sides of SnO₂ and ZnO. This results in the formation of smaller channel width (W₂) and hence increase in the resistance. Therefore, the enhanced electrical response of the nanorod sensor to NO₂ gas was found. In addition to the

depletion layer, a potential barrier with height E₂ also forms at both sides of the interface. The potential barrier E₂ is higher than E₁, a larger potential modulation takes place in the presence of gas and hence an enhanced electrical response of the nanorod sensor to NO₂ gas was reported.

In 2017, Qin et al. developed a unique surface etching method of ZnO micro/nanowire which had led to an increase in the sensitivity, response and recovery time [33]. The etching of the microwire surface area leads to an increase in the surface density of single ionized oxygen vacancies and specific surface area and hence the increase in the adsorption sites for gas molecules. This surface etching ultimately results in an increase in sensitivity by about ~20%. Under the influence of UV light of 148.8 mW/cm², the sensitivity of the sensor further increased to 411% and recovery and response time decreased to ~2% and ~20% under dark and light conditions, respectively. The surface etching method of microwire of ZnO leads to an increase in the sensitivity from 3.6% to 71.8% in the presence of 20 ppm of NO₂. By controlling the etching time, the sensitivity of the sensor can be controlled. The ZnO MW based sensor showed an increase in the sensitivity and reduction in response and recovery time under UV illumination at room temperature.

In the following year 2018, Betty et al. proposed a highly selective gas sensor based on a hybrid structure of porous silicon and ZnO [36]. The chemically processed ZnO nanoparticles were drop casted upon single crystalline silicon (p-type) substrate (Si) and also on electrochemically processed p-type porous silicon (PS). At room temperature, the PS-ZnO sensor showed an increase in the current for NO₂ gas while there was no significant change in the presence of other oxidizing and reducing gases. The sensor displayed a response time of 50 s while the sensitivity of 35% in the presence of 200 ppb of NO₂ at 25 °C. The temperature dependence was also studied and it was found that the suitability of the sensor is up to 60 °C only. The PS-ZnO sensor showed a maximum response to NO₂ gas while very less response to NH₃ and SO₂. Two different heterostructures, i.e., planar silicon-ZnO (Si-ZnO) and ZnO on electrochemically processed porous silicon (PS-ZnO) were prepared. The gas sensitivity of PS-ZnO sensor is extremely high to NO₂ in ppb range with high specificity while Si-ZnO sensor has higher sensitivity with precise responses to NH₃ and SO₂.

In the same year, Yu et al. proposed a highly sensitive NO₂ gas sensor based on the heterostructures of ZnO-rGO [121]. The soft solution and thermal reduction processes were used for fabricating ZnO nano-walls modified with rGO nano-sheets. The ZnO layer was homogeneously deposited on the surface of rGO. The sensing performance of the developed sensor was studied. At room temperature, the authors observed an increase in the electrical carrier concentration from $0.04 \times 10^{15} \text{ cm}^3$ to $3.148 \times 10^{15} \text{ cm}^3$ and decrease in the electrical

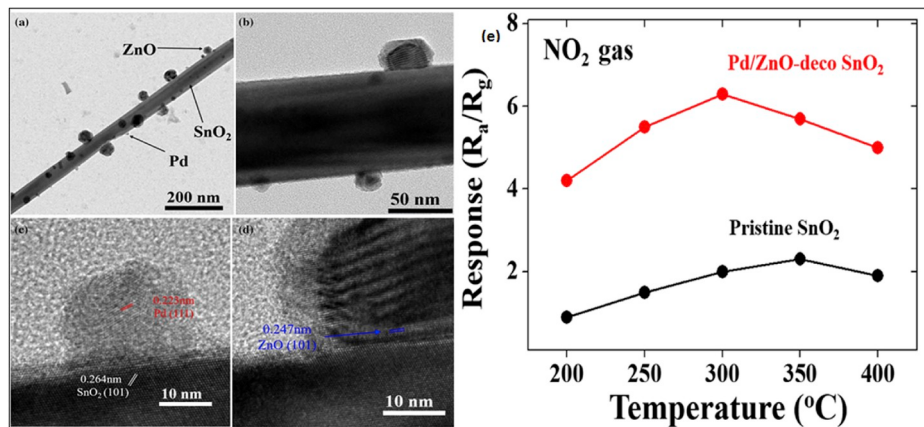


Fig. 14. (a) Low magnification TEM images of Pd/ZnO-SnO₂, (b) Medium resolution TEM of Pd/ZnO-SnO₂, (c) High-resolution TEM of Pd/ZnO decorated SnO₂, (d) corresponding electron diffraction of co-decorated ZnO/Pd on SnO₂ surface, (e) The temperature dependence on the sensor in case of both pristine SnO₂ and Pd/ZnO-SnO₂. Copyright permission from Ref. [130].

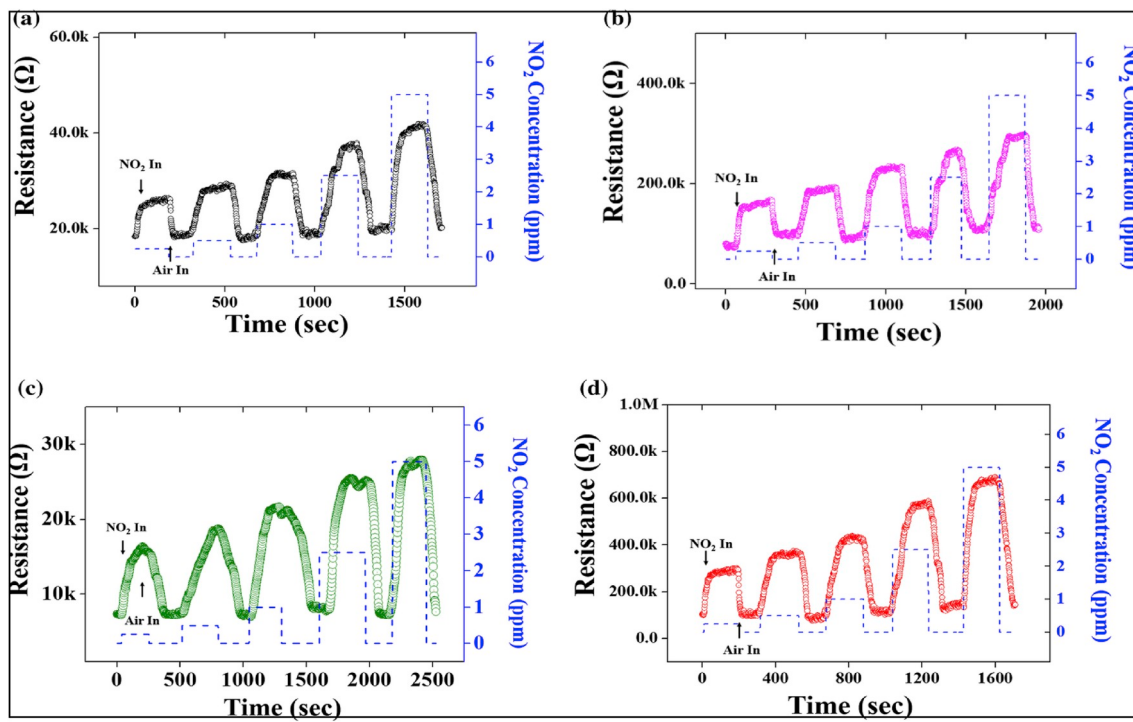


Fig. 15. The dynamic sensing response of different sensor in the existence of NO₂ gas at 300 °C. (a) the response of pure SnO₂ nanorods, (b) the response of ZnO decorated SnO₂ nanorods, (c) the response of Pd decorated SnO₂ nanorods, (d) and the response of Pd/ZnO co-decorated SnO₂ nanorods. Copyright permission from Ref. [130].

resistances from 998.8.cm⁻¹ to 16.01.cm⁻¹ for the ZnO-rGO heterojunction. It was also found that the ZnO-rGO heterojunction exhibited good sensitivity, selectivity and response to NO₂ gas. The remarkable connection between a 3D planar network of ZnO nanowalls with porous nature and rGO is responsible for the enhancement in the performance of ZnO-rGO heterostructures at room temperature in comparison with ZnO nanowalls or rGO. Also, the as-developed ZnO-rGO heterostructures at room temperature have good repeatability and stability. In the ambient atmosphere, the oxygen molecules adsorbed on the surface of ZnO and ionized to O⁻ by capturing free electrons from the ZnO, result in the variation of sensor resistance. When exposed to NO₂ gas, the adsorbed NO₂ gas molecules will capture the electrons from ZnO surface as it has higher electron affinity than pre-adsorbed oxygen. Hence, the overall resistance increases when exposed to NO₂ gas. In case of heterostructures of ZnO-rGO, the fermi level of n-ZnO (5.20 eV) being higher than rGO (4.75 eV), allows charge transfer from rGO to the conduction band of ZnO, further increasing the adsorption of NO₂. Hence, the increase in the sensitivity can be attributed to the electron transfer between rGO and ZnO.

Another group in 2018, developed a visible ultraviolet (UV) photodetector based on ZnO nanorod which is highly sensitive and selective towards NO₂ gas [122]. The sensing material ZnO nanorod was obtained by using a two-step chemical method. The large surface area for sensing mechanism was provided by well-aligned one dimensional (1D) network of ZnO nanorods. The UV photodetector in A region (364.81 A/W) possess fast photo-switching analysis at 5 V bias voltage and high responsivity. It shows the junction formed between metal and semiconductor is good ohmic contact. The sensing performance of ZnO nanorods was monitored at a temperature of about 175 °C. The maximum sensing response at 40 ppm of NO₂ was found to be 35. The ZnO nanorod detector also shows high selectivity for NO₂ gas. Good repeatable characteristics of the as-developed sensor can be seen at the lower concentration of 2 ppm of NO₂. Simple and cost-effective sensor technology was employed for developing extremely ordered ZnO nanorod as highly sensitive NO₂ sensor and highly sensitive UV

photodetector.

The recent advancement in the material refining methods has allowed scientists to explore research and record the properties of nanostructured metal oxides. One of the better options is the multitude application of ZnO. In this regard, Vanalakar et al. employed a hydrothermal route for synthesizing ZnO nanorods for an enhanced sensing response towards NO₂ gas at low temperature [127]. In this paper, the hydrothermal method is used for developing ZnO on the silicon substrate and both chemical and physical properties were thoroughly characterized. Different samples were obtained with different concentrations of zinc nitrate. FESEM images revealed the formation of vertically aligned ZnO nanorods by hydrothermal method. Also, with increasing concentration of zinc nitrate, nanorods become denser and grow larger in size. However, as compared with other samples, the ZnO-d becomes slightly shorter. They observed that the prepared ZnO nanorods are vertically aligned and show the wurtzite type structure. The PL analysis of as-prepared sample confirms the presence of defects. These defects come into picture due to the oxygen vacancy concentration. These defects in conjunction with a high surface area of the nanorods and optical inter rod spacing create conditions for high adsorption and diffusion. The developed ZnO gas detector exhibited a superior response of about 570 for 100 ppm NO₂ at 150 °C. Along with high sensing response, the ZnO sensor also exhibits high selectivity at a lower temperature.

Recently, V.B. Patil et al. developed an outstanding sensor with a high response, fast response and recovery, high stability and reproducibility based on heterostructure of ZnO NWs-CuO nanoparticles [119]. The design of the device technology working at low temperature with high sensitive performance using heterostructure materials is very crucial. The sensors were named as NWA and NWG after thermal evaporation process via annealing in air and argon, respectively. The topology at various magnifications of ZnO–CuO heterostructure clearly shows the creation of ZnO–CuO heterostructure between n-type ZnO and p-type CuO NPs. Also, surface morphology study revealed well-aligned porous nature of NWG-type ZnO–CuO heterostructures in contrast to

NWA heterostructures. The high surface-to-volume ratio of the NWs type morphology is beneficial for gas detection. The developed heterostructures of ZnO–CuO showed remarkable response to NO₂ gas having fast response and recovery, high stability, high response, and outstanding reproducibility. The general gas sensing mechanism of metal oxides semiconductor is well understood. In the case of heterostructures of ZnO–CuO, the sensing comes from the top of the ZnO layer and depletion layer formed between ZnO and CuO. In an ambient atmosphere, oxygen gets adsorbed on the surface of the depletion layer in the forms of O, O^{2−}, O₂[−] by accepting electrons from the surface matrix. Also, the positioning of the ZnO NWs on the top of CuO NPs is advantageous to enhance the response towards NO₂ due not only to increased surface-to-volume ratios but also to a spatially heterogeneous surface matrix, as such type of matrix is appropriate for improved adsorption/desorption of NO₂ gas molecules.

2.2.2. Miscellaneous metal oxide-based NO₂ gas sensors

In 2018, Fu et al. adopted a facile two-step synthesis approach was used to synthesize actinomorphic flower-shaped core-shell structured ZnO–ZnFe₂O₄ composites for an enhanced gas sensing response [34]. In analogy with pure ZnO, the flower-shaped ZnO–ZnFe₂O₄ composite was found to be highly sensitive, with shorter recovery and response times and more selective to a low concentration of NO₂ at an operating temperature of 200 °C. The XRD analysis of the composite confirmed the wurtzite ZnO structure and also the residual peak attributed to the spinel ZnFe₂O₄ structure. The highly crystalline nature of ZnO–ZnFe₂O₄ composites was indicated by the sharp and narrow diffraction peaks. The deficiency of any other peak confirms the purity of ZnO–ZnFe₂O₄ composites. The sensing mechanism of ZnO–ZnFe₂O₄ based sensor can be attributed to the flower-like core-shell structure and the formation of p-n heterojunction at the interface of ZnO and ZnFe₂O₄ composite. In the presence of ambient air, oxygen adsorbs on the surface and two conjugated electron depletion layers are formed on the surface of ZnFe₂O₄ nanoparticles and the interface between ZnO and ZnFe₂O₄. The adsorbed oxygen molecules (O, O₂[−], O^{2−}) not only capture electrons from the ZnFe₂O₄ shell but also capture electrons from ZnO core, making ZnO–ZnFe₂O₄ based sensor highly resistive in comparison to pure ZnO. When a highly oxidizing NO₂ gas is exposed to the heterostructures of ZnO–ZnFe₂O₄, the NO₂ gas acts as an electron acceptor to capture more electrons due to their high electron affinity than that of oxygen, leading to the remarkable increase of the sensor resistance and electron depletion width. This result makes the actinomorphic flower-shaped ZnO–ZnFe₂O₄ composites a perfect contender for NO₂ gas sensing.

In the same year, Sheng et al. developed a gas sensor for room temperature NO₂ detection under UV light based on ZnO-silk fibroin (ZnO/SF) using hydrothermal method [35]. The UV light-activated sensor was efficient and able to trace NO₂ gas very fast at RT. Under the influence of UV light of 365 nm, the ZnO-SF detector demonstrated the response of 85 and average recovery and response time of 16 s and 26 s, respectively towards 20 ppm of NO₂ at RT. Also, the as-developed ZnO-SF sensor showed excellent linearity in response toward NO₂ at RT under UV illumination. The SEM investigation validated the existence of small block-shaped and small particles while XRD investigations indicated the existence of wurtzite ZnO structure and the absence of any impurities.

Gosavi et al., in 2017 provided a breakthrough in the field of ZnO metal oxide-based gas sensors with high sensitivity towards NO₂ gas. They developed flower-shaped ZnO thin films for resistive sensing of NO₂ gas [32]. A cost-effective, soft chemical solution synthesis technique was employed for uniform deposition of jasmine flower-shaped thin films. X-ray diffraction study of the ZnO revealed the hexagonal wurtzite structure. It was also found that at all deposition temperatures, a large jasmine flower-shaped structure of ZnO is uniformly maintained. The elemental investigation of the sample confirms the presence of Zn and O with no impurities. The combined analyses of Raman spectroscopy, resistivity analysis and elemental analysis confirmed the presence

of oxygen vacancies and wurtzite structure of ZnO. The as-grown jasmine flower-shaped ZnO thin film based detector exhibits a high sensitivity towards 10 ppm of NO₂ with rapid recovery and fast response time of 54 s and 65 s, respectively.

A sol-gel method was used for developing ZnMgO thin films for studying structural, NO₂ gas sensing and optical properties [123]. The sol-gel processed thin films of ZnO and ZnMgO was spin-coated on a glass substrate. The thin film ZnMgO absorption spectra analysis shows a bandgap variation from 3.19 to 3.36 eV which agrees well with PL emission measured at low temperatures. The gas sensing measurements of the ZnMgO samples were performed in air containing 100 ppm of NO₂. The incorporation of magnesium into ZnO leads to decreased sensor response towards NO₂. However, on increasing the concentration of magnesium in the sample, the response and recovery times drop significantly.

In another approach, Patil et al. prepared a highly selective NO₂ gas sensor with a low detection limit. Thin films of ZnO were synthesized using sol-gel and spin coating procedures for detecting NO₂ gas [124]. The sensing performance of as-prepared ZnO thin films towards different gases, e.g., H₂S, CH₃OH, NO₂, Cl₂ and NH₃ were studied at various operating temperatures. At a temperature of 200 °C and 100 ppm of NO₂, the as-developed ZnO thin film sensor exhibited a response of 12.3. The as-processed ZnO thin film sensor depicted a highly selective response to NO₂ gas besides the detector is capable of detecting NO₂ concentration as low as 5 ppm with a response of 4.1. Most of the metal oxide-based gas sensors detect gas at high operating temperatures. This requires an additional requirement of heating the sample in order to attain the detection temperature. The thermal treatment of the sensor produces oxygen which plays a vital role in gas sensing mechanism. The oxygen molecules adsorb on the surface and grain boundary of the metal oxide sensor to create a depletion region. The adsorbed oxygen changes into O^{2−} ions by capturing electrons from the metal surface. This increases the number of electrons in the sensing layer.

Katz et al. fabricated a hybrid structure combining a polymer with metal oxide which provides high sensing response to NO₂ gas. The hybrid structure, i.e., P3HT-ZnO@GO composite, was obtained from zinc oxide-graphene oxide (ZnO@GO) and (P3HT) poly (3-hexylthiophene) nanoparticles [125]. The ionic aggregation was used to prepare core-shell nanostructure particles of zinc oxide (ZnO) and graphene oxide (GO). The organic field-effect transistors (OFETs) for gas sensing were fabricated by spin coating the prepared mixtures of ZnO@GO and P3HT on the oxide deposited silicon substrate. The gas sensing properties of the developed composite structures of ZnO@GO and P3HT composite as semiconducting material for OFETs were investigated in the presence of nitrogen dioxide (NO₂) gas. In comparison with pure P3HT, the developed hybrid P3HT-ZnO@GO composite has sensing response up to 210% under the exposure of 5 ppm of NO₂ gas. As the amount of weight fraction of ZnO@GO rises, the sensing response of the sensor also increases accordingly at RT. The sensor response was also found to increase with the increase in exposure time and NO₂ concentration.

In 2018, Tian et al. proposed another approach in which multilayered black phosphorus (m-BP) was incorporated in ZnO, forming composite structures of ZnO-BP which exhibit outstanding selectivity, higher response as well as rapid response behaviour [126]. In hollow spheres of zinc oxide (ZnO) the multilayers of black phosphorus (m-BP) were effectively incorporated and the resultant composite structure was named as ZnO-BP. The incorporation of BP into ZnO-BP composite leads to the large surface area, enhanced charge transfer and excellent carrier mobility in comparison with BP, graphene and ZnO based sensors. The developed ZnO-BP composite sensor exhibits the ultra-high sensing limit, i.e., 1 ppb of NO₂ gas.

Recently, Aziz et al. developed an advanced approach for synthesizing polycrystalline, self-supporting ZnO nanofibers, which are capable of detecting very low levels of NO₂ [128]. The developed

polycrystalline ZnO is able to detect 1 part per billion (ppb) of NO₂ gas. The core-shell electro-spinning of the inorganic metal precursor such as zinc neodecanoate is used for creating ZnO nanofibers for NO₂ detection. The use of this new and innovative method resulted in the formation of self-supporting, contamination-free, polycrystalline ZnO nanofibers with average grain size and diameter of 8 and 50 nm, respectively. These properties are ideal for gas sensing purposes. The core-shell electro-spinning method used in this paper is very cost-effective and can be easily scaled. The sensitivity of the device can be enhanced by employing interdigitated electrodes and aligned electrospun fibres. This simple technique can be easily used for various metal precursor solutions, thereby assisting the formation of other metal oxides. The functionalities and properties of these materials could be very useful in many fields including energy generation and storage, sensing and wearable technologies. The polycrystalline nature of synthesized ZnO and the presence of nanograins may be suitable for application in spintronics where ferromagnetism in ZnO has been associated with the ZnO grain boundaries; other uses may comprise syngas cleansing water and air.

In a unique approach, the assembly of the smallest nanoparticles with mesoporous ZnO sheets was obtained which depicted a high response at room temperature towards NO₂ gas. Wang et al. constructed small nanoparticles to develop mesoporous ZnO sheets using facile synthesis for increased NO₂ gas detection at RT [129]. At low temperature such as 100 °C, calcination of δ -Zn(OH)₂ precursor was performed for facile synthesis of nanoparticles assembled mesoporous ZnO sheets. Ultrasmall ZnO nanoparticles with a high surface area of 87.63 m² g⁻¹ and an average crystal size less than 10 nm were assembled for developing mesoporous ZnO sheets. The enhancement in the sensitivity response of the sensor towards NO₂ gas can be accredited to the high surface area, oxygen vacancies and rich mesopores which facilitate the diffusion and adsorption of NO₂ molecules. The assembly of nanoparticles to obtain mesoporous ZnO sheets depicted a high response of about 135% at room temperature towards 1 ppm NO₂. Also, the developed sensors exhibited full reversibility, good selectivity towards NO₂ and superior recovery/response times. The nanoparticles of ZnO with small crystal size increases radical modulation in the conduction channel for NO₂ gas sensing operations.

In 2018, Yi et al. developed a method for increasing the sensing area to enhance sensitivity. Synthesis of ZnO-SnO₂ composite was done by a

facile solvothermal method in order to decorate ZnO onto SnO₂ microspheres [31]. The study displayed that the developed sensor was highly sensitive to NO₂ gas molecules. It was found that in comparison with pure SnO₂ microspheres, ZnO-SnO₂ microspheres based sensor response was 3 times higher at optimum temperature towards 100 ppm of NO₂. The recovery and response time was also reduced remarkably. The increase in the sensitivity is attributed to the extra area available for adsorption of NO₂ molecules provided by ZnO decoration. The SEM images obtained clearly show the porous structure of SnO₂ microspheres (see Fig. 16). The deposition of ZnO on SnO₂ completely retains the porous structure of pristine SnO₂ without any disturbance on the structure. They observed the coexistence of both ZnO and SnO₂ particles and the tetragonal structure of SnO₂ (See Fig. 16).

Verma et al. developed a highly selective NO₂ gas sensor by synthesizing a ternary complex of CuO-ZnO/rGO from ZnO nanosheets and CuO 1D nano chains, which were synthesized via reflecting and wet chemical method, respectively [131]. The influence of individual ZnO and CuO material composition on the sensing behaviour of the composites of CuO-ZnO/rGO towards NO₂ gas have been investigated. The drop-casting method is used for synthesizing composites of CuO-ZnO/rGO with different concentrations of both ZnO and CuO on glass substrates. It was found that at room temperature (RT), the developed hybrid CuO-ZnO/rGO with a composition (CuO: ZnO = 1:1) have a sensitivity of ~62.9 towards NO₂ of 40 ppm concentration. In comparison with ZnO/rGO and CuO/rGO sensors, the composite sensor CuO-ZnO/rGO sensitivity towards NO₂ gas is 1.3 and 3.1 times higher respectively. The developed composite sensor is highly selective towards NO₂ gas and moreover, this sensor shows good stability for a period of 5 weeks.

Wang et al. developed a unique approach for enhancing the sensitivity, response and recovery speed of the sensor to many folds. For achieving a mentioned enhancement in sensor characteristics, they simply annealed the sensor at high temperature. The highly sensitive gas sensor for detecting ppb levels of NO₂ at low operating temperature was made by In₂O₃ nanobricks [132]. Oil bath storm and consequent calcination process without any surfactants or templates were used for synthesizing brick-like In₂O₃ nanomaterials. Internal defect structures and surface states of the material can be influenced by the different temperatures of calcination process. The influence of internal defects and

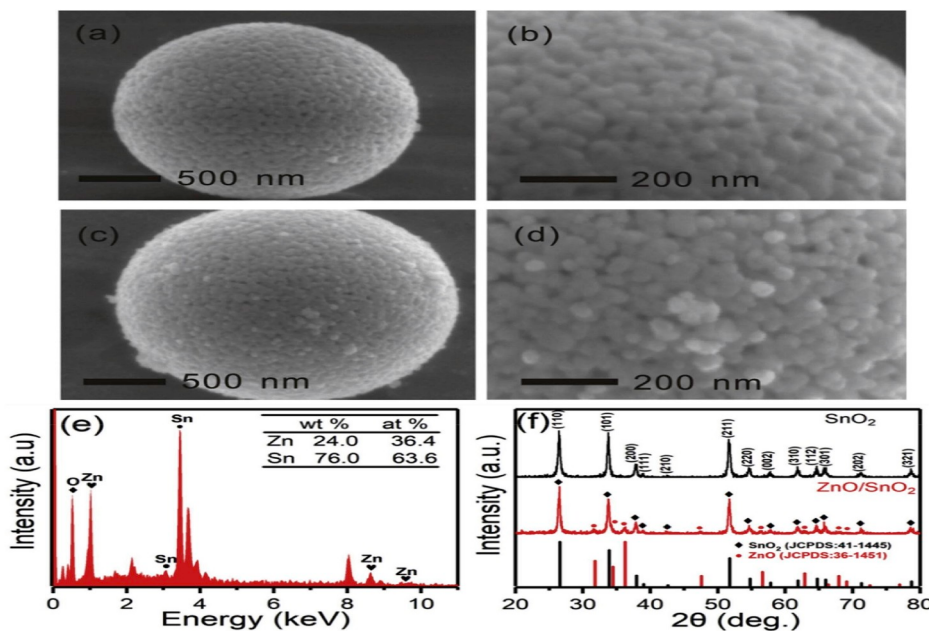


Fig. 16. (a) & (b) Typical SEM photographs of pure SnO₂ microspheres. (c) & (d) SEM photographs of ZnO-SnO₂ hybrid material microspheres. (e) ZnO-SnO₂ composites EDX spectrum. (f) Pristine SnO₂ and ZnO-SnO₂ composite XRD pattern comparison. Copyright permission from Ref. [31].

material surface states on gas sensing is illustrated by XPS and photoluminescence spectra (PL). It was found that the 400 °C annealed In₂O₃ nanomaterial sample has a high sensing response of 402 towards 500 ppb NO₂ gas with fast recovery and response time at relatively low performing temperature of 50 °C. Also, the sensor has a great stability period of over 30 days and a good linear response. The reasons for such superior gas sensing properties can be accredited to good electrical properties, large surface area and sufficient chemically adsorbed oxygen. The developed In₂O₃ sensor outperforms many other works on NO₂ gas sensing based on hybrids of In₂O₃ [133–136].

Table 2 enlists the performance parameters such as preparation method, structure, materials used, the concentration of NO₂ gas, response and recovery times, and operating temperature for NO₂ gas sensors based on various oxide nanostructures and their hybrids.

2.3. Graphene-based nanostructures

The addition of reduced graphene oxide (rGO) into SnO₂ not only improved the response and recovery speeds but the response of the sensor also increases with temperature. Wang et al. developed a composite of rGO and SnO₂ nanoparticles for enhanced NO₂ gas sensing [137]. A hydrothermal method with facile one-pot microwave assistance was used for obtaining rGO/SnO₂ composites. The optimal operating temperature for both rGO/SnO₂ composite and pure SnO₂ were found to be 75 and 65 °C, respectively. The peak response for the rGO/SnO₂ composite sensor was found to be 227.6 while in case of pure SnO₂ sensor response was 34.6 for 350 ppb of NO₂ gas. Temperature greatly affects the surface reactions and thus, can be responsible for the temperature-dependent property of the sensor. The sensing gas particles (e.g., NO₂) fail to interact with oxygen species pre-adsorbed on sensor surface at lower temperatures owing to inadequate thermal energy. The sensor responses considerably increases with increase in temperature as the gas particles attain sufficient thermal energy to overcome the activation energy boundary of surface reactions. However, with further increase in temperature, the response is limited by difficulties in gas adsorption and low utilization rate of the sensing layer [138]. The utilization rate and the gas adsorption were found to be in balance at 75 °C, resulting in a maximum response of the composite sensor at this temperature. The addition of rGO helps in improving both recovery and response speeds. In case of pure SnO₂ sensor, the recovery and response time were 54.7 and 39.2 min, respectively; which in case of rGO/SnO₂ composites were 1 and 6.5 min, respectively. The increase in surface area of rGO/SnO₂ composites due to the addition of rGO leads to the increase in sensitivity of the sensor.

Flexible sensors hold great promise for various innovative applications in fields such as environment, medicine, biology and most importantly, healthcare. Considering the fact that most of the healthcare electronics, wearable systems and laboratory on-chip testing tools can be expected to come in contact with arbitrarily curved interfaces, the flexibility of the sensor is essential for improving the interactions. Zhang et al. reported a flexible sensor based on direct laser writing technology (DLW) for the fabrication of composite films of graphene oxide (GO) and In₂O₃ for NO₂ sensing flexible arrays working at RT [139]. The photo-reduction of GO is achieved by laser treatment which led to the creation of porous structure allowing the removal of oxygen groups. The laser treatment also enables mask free patterning in a programmable manner, resulting in the assimilation of flexible sensor arrays on any substrates. In general, both In₂O₃ and GO are not conductive and hence the composite In₂O₃@GO is insulating in nature with resistance found to be $\sim 7.6 \times 10^8 \Omega$. Laser treatment of the In₂O₃@GO composites decreases the resistance to $\sim 230 \Omega$. Under the controlled environment, the sensitivity of rGO based sensor is low in comparison to the sensitivity of In₂O₃@GO composites. The developed In₂O₃@GO composite sensor showed an admirable selectivity toward NO₂ gas and offers a linear dependence to the NO₂ concentration [140].

Ching-Ting et al. developed a membrane-based gas sensor. One

advantage of membrane-based gas sensors is their applicability for differing gas components. A highly sensitive NO₂ gas sensor using rGO and ZnO membrane was developed [141]. In addition, an installed sensor cell can be calibrated without dismounting under an unknown background concentration. The GO-ZnO complex films were processed by coating the GO-ZnO solution on glass substrates. The rGO-ZnO composite films were obtained by removing the oxygen-containing functional groups residing on GO-ZnO composite by employing a thermal annealing method. In comparison to rGO and ZnO sensing membrane, the sensitivity of the rGO-ZnO film is better and the reason for this increase in composite sensor response can be accredited to the elimination of oxygen-containing functional groups. The increase in sensitivity of rGO-ZnO composite films can be accredited to the structure of C–O–Zn bonds and supply of electrons from the oxygen vacancies of ZnO material. The effect of GO/ZnO ratio on the sensing performance was also studied where 0.08 was found to be the optimized ratio. The various parameters for the rGO-ZnO composite sensor such as response time, sensing responsivity and recovery time were found to be 6.2 min, 47.4% and 15.5 min, respectively for 100 ppm NO₂ environment at RT. In the case of rGO sensor, the response time, sensor responsivity and recovery time were 10.3 min, 19.0% and 75.9 min, respectively. The detection limit for the composite sensor was found to be 5 ppm with linear sensing responsivity from 10 ppm to 100 ppm.

Zhang et al. reported the impact of oxygen-containing groups on the rGO based NO₂ gas sensor at room temperature [142]. The modified hummers method was employed to obtain graphene oxide (GO). Hydrothermal reduction method was used to obtain a series of rGO from the graphene oxide at oxidation temperatures of 65–95 °C. The sensitivity of the sensor first increases with a rise in the oxidation temperature of GO and then decreases with the further increase in the temperature. The rGO sample obtained by the oxidation of GO at 85 °C exhibited the highest sensitivity of 36.7% at 5 ppm of NO₂ at RT. This increase in sensitivity of the sample oxidized at 85 °C can be accredited to the presence of C–O bonds in large number in the sample. It has already been reported that the sheet edges of rGO are occupied by carboxyl and carbonyl groups, while the basal plane is occupied by epoxy and hydroxyl groups at both sites [143,144]. The rGO edges occupied by carbonyl group and vertical to the basal plane is occupied by hydroxyl group which possess higher adsorption energies –0.504 eV and –0.238 eV than the other functional groups and it is more important for adsorption of NO₂ gas molecules. Hence the sensitivity of the rGO sensor depends on the presence of several C–O bonds.

Richard et al. proposed a unique material to enhance the sensitivity of NO₂ gas sensors, i.e., TiO₂. A sol-gel technique was employed to synthesize both pure TiO₂ and graphene/TiO₂ hybrid to monitor and neutralize the effects of NO₂ gas [145]. The hybrid structure of graphene/TiO₂ was obtained by the addition of graphene in the reaction vessel before the beginning of the sol-gel reaction followed by annealing (GTiO₂S). In another method, the graphene was added to already annealed TiO₂ nanoparticles (GTiO₂M). GTiO₂S derived sensor exhibited more sensing response than the sensor fabricated from GTiO₂M. In the presence of low power UV illumination, the sensor showed strengthened response to 1750 ppb of NO₂ which is two-fold the response in dark. The detection limit of the sensor was found to be 50 ppb of NO₂. In comparison to other NO₂ sensors based on TiO₂ which work at high temperatures, the gas sensor based on GTiO₂S works at RT. Also, the detection limit for GTiO₂S is lower (in ppb level) with a short response and recovery times.

3. Conclusions and perspectives

The gas sensor fabrication has experienced a radical transformation into a thin film from powder-based thick films formed by chemical and physical vapor deposition techniques. Both deposition techniques facilitate the use of porous structures which are relevant for gas sensing and also help in controlling the material microstructures such as grain

boundary and size. Literature survey on materials for gas sensor helps us in identifying the major three different classes of materials which are essential for gas sensing. The three classes of materials are 2D transition metal dichalcogenides (TMDs), oxide nanostructures, and graphene composites which have undoubtedly proven their potential for spontaneous sensing of toxic and dangerous gases and under controlled condition, the real-time gas observation. In spite of all this, there are some relevant disadvantages to these materials, which leave room for further improvements to enhance stability and selectivity. Moreover, in the case of both graphene and TMDs, the gas detection mechanism is still not well settled. The design of heterostructures and surface functionalization with a variety of nanomaterials can overcome these disadvantages in the near future. In summary, the TMDs nanosheets with their rare attributes coupled with substantial production have excited tremendous research efforts to exploit them as building blocks for structurally important functional composite nanomaterials. The formation of innovative functional hybrids of TMDs has been accomplished by conjugation of transition metals and chalcogen atoms. In this survey, we have studied the latest development in the TMDs and metal oxide nanostructures based NO₂ gas sensors and the summary is given in two tables. Along with the advancement of modern approaches, one of the utmost encouraging chances in this area is the hybridization of other kinds of TMDs nanostructures such as ZrS₂, WS₂, HfS₂, and WSe₂ with a range of materials to achieve innovative functional composites for numerous operations.

Declaration of competing interest

There is no conflict of interest.

Acknowledgements

The investigation was supported by the Ministry of Science and Higher Education of Russian Federation (project 0777-2017-0009)

Appendix A. Supplementary data

Supplementary data to this article can be found online at <https://doi.org/10.1016/j.mssp.2019.104865>.

References

- [1] W.H. Organization, World Health Statistics, 2018: Monitoring Health for the SDGs Sustainable Development Goals, World Health Organization, 2018.
- [2] T.W. Hesterberg, W.B. Bunn, R.O. McClellan, A.K. Hamade, C.M. Long, P.A. Valberg, Critical review of the human data on short-term nitrogen dioxide (NO₂) exposures: evidence for NO₂ no-effect levels, *Crit. Rev. Toxicol.* 39 (9) (2009) 743–781.
- [3] B. Bhagare, N.S. Ramgir, S. Jagtap, A.K. Debnath, K.P. Muthe, C. Terashima, D.K. Aswal, S.W. Gosavi, A. Fujishima, XPS and Kelvin probe studies of SnO₂/RGO nanohybrids based NO₂ sensors, *Appl. Surf. Sci.* 487 (March) (2019) 918–929.
- [4] M.L. Wong, B.D. Charnay, P. Gao, Y.L. Yung, M.J. Russell, Nitrogen oxides in early earth's atmosphere as electron acceptors for life's emergence, *Astrobiology* 17 (10) (2017) 975–983.
- [5] D.S. Jyethi, in: U. Kulshrestha, P. Saxena (Eds.), Plant Responses to Air Pollution, Springer Singapore, Singapore, 2016, pp. 5–19, https://doi.org/10.1007/978-981-10-201-3_2.
- [6] S.M. Bernard, J.M. Samet, A. Grambsch, K.L. Ebi, I. Romieu, *Environ. Health Perspect.* 109 (2001) 199–209.
- [7] B.J. Finlayson-Pitts, J.N. Pitts Jr., Chemistry of the Upper and Lower Atmosphere: Theory, Experiments, and Applications, Academic press, 1999.
- [8] G. Korotcenkov, The role of morphology and crystallographic structure of metal oxides in response of conductometric-type gas sensors, *Mater. Sci. Eng. R Rep.* 61 (2008) 1–39.
- [9] P.G. Han, H. Wong, M.C. Poon, Sensitivity and stability of porous polycrystalline silicon gas sensor, *Colloid. Surf. A Physicochem. Eng. Asp.* 179 (2001) 171–175.
- [10] A. Zandi, A. Gilani, H. Ghafoori fard, J. Koohsorkhi, An optimized resistive CNT-based gas sensor with a novel configuration by top electrical contact, *Diam. Relat. Mater.* 93 (January) (2019) 224–232.
- [11] H. Jeong, Y. Noh, D. Lee, Highly stable and sensitive resistive flexible humidity sensors by means of roll-to-roll printed electrodes and flower-like TiO₂ nanostructures, *Ceram. Int.* 45 (1) (2019) 985–992.
- [12] A. Mirzaei, et al., An overview on how Pd on resistive-based nanomaterial gas sensors can enhance response toward hydrogen gas, *Int. J. Hydrogen Energy* 44 (36) (2019) 20552–20571.
- [13] J.M. Walker, S.A. Akbar, P.A. Morris, Synergistic effects in gas sensing semiconducting oxide nano-heterostructures: a review, *Sens. Actuators B Chem.* 286 (December 2018) (2019) 624–640.
- [14] G. Korotcenkov, V. Brinzari, B.K. Cho, In₂O₃- and SnO₂-based ozone sensors: design and characterization, *Crit. Rev. Solid State Mater. Sci.* 43 (2) (2018) 83–132.
- [15] L. Yu, et al., Hierarchical 3D flower-like MoS₂ spheres : post-thermal treatment in vacuum and their NO₂ sensing properties, *Mater. Lett.* 183 (2016) 122–126.
- [16] W. Yan, M.A. Worsley, T. Pham, A. Zettl, C. Carraro, R. Maboudian, Effects of ambient humidity and temperature on the NO₂ sensing characteristics of WS₂/graphene aerogel, *Appl. Surf. Sci.* 450 (2018) 372–379.
- [17] Y. Zhang, W. Zeng, Y. Li, Hydrothermal synthesis and controlled growth of hierarchical 3D flower-like MoS₂ nanospheres assisted with CTAB and their NO₂ gas sensing properties, *Appl. Surf. Sci.* 455 (May) (2018) 276–282.
- [18] M. Wook, S. Myeoung, K. Nam, K. An, B. Ku, Highly transparent and flexible NO₂ gas sensor film based on MoS₂/rGO composites using soft lithographic patterning, *Appl. Surf. Sci.* 456 (June) (2018) 7–12.
- [19] S. Zhao, G. Wang, J. Liao, S. Lv, Z. Zhu, Z. Li, Vertically aligned MoS₂/ZnO nanowires nanostructures with highly enhanced NO₂ sensing activities, *Appl. Surf. Sci.* 456 (June) (2018) 808–816.
- [20] M. Donarelli, et al., Response to NO₂ and other gases of resistive chemically exfoliated MoS₂ -based gas sensors, *Sens. Actuators B Chem.* 207 (2) (2015) 602–613.
- [21] A. Kumar, S. Kumar, A convenient and efficient copper-catalyzed synthesis of unsymmetrical and symmetrical diaryl chalcogenides from arylboronic acids in ethanol at room temperature, *Tetrahedron* 70 (9) (2014) 1763–1772.
- [22] Y.S. Shim, et al., Synthesis of numerous edge sites in MoS₂via SiO₂Nanorods platform for highly sensitive gas sensor, *ACS Appl. Mater. Interfaces* 10 (37) (2018) 31594–31602.
- [23] E. Lee, Y.S. Yoon, D.J. Kim, Two-dimensional transition metal dichalcogenides and metal oxide hybrids for gas sensing, *ACS Sens.* 3 (10) (2018) 2045–2060.
- [24] H. Medina, et al., Wafer-scale growth of WSe₂ monolayers toward phase-engineered hybrid WO_x/WSe₂ films with sub-ppb NO_x gas sensing by a low-temperature plasma-assisted selenization process, *Chem. Mater.* 29 (4) (2017) 1587–1598.
- [25] E. Núñez Carmona, et al., Detection of food and skin pathogen microbiota by means of an electronic nose based on metal oxide chemiresistors, *Sens. Actuators B Chem.* 238 (2017) 1224–1230.
- [26] H.K. Hong, C.H. Kwon, S.R. Kim, D.H. Yun, K. Lee, Y.K. Sung, Portable electronic nose system with gas sensor array and artificial neural network, *Sens. Actuators B Chem.* 66 (1) (2000) 49–52.
- [27] S. Chen, Y. Tang, K. Zhan, D. Sun, X. Hou, Chemiresistive nanosensors with convex/concave structures, *Nano Today* 20 (2018) 84–100.
- [28] X. Chen, et al., NO₂ sensing properties of one-pot-synthesized ZnO nanowires with Pd functionalization, *Sens. Actuators B Chem.* 280 (2) (2019) 151–161.
- [29] Y. Chen, et al., Two-dimensional metal nanomaterials: synthesis, properties, and applications, *Chem. Rev.* 118 (13) (2018) 6409–6455.
- [30] O. Lupon, V. Postica, F. Labat, I. Ciofini, T. Pauperté, R. Adelung, Ultra-sensitive and selective hydrogen nanosensor with fast response at room temperature based on a single Pd/ZnO nanowire, *Sens. Actuators B Chem.* 254 (2018) 1259–1270.
- [31] Z. Li, J. Yi, Synthesis and enhanced NO₂-sensing properties of ZnO-decorated SnO₂ microspheres, *Mater. Lett.* 236 (2) (2019) 570–573.
- [32] Y.N. Rane, et al., Synthesis of flower shaped ZnO thin films for resistive sensing of NO₂ gas, *Microchim. Acta* 184 (7) (2017) 2455–2463.
- [33] L. Meng, et al., Enhancing the performance of room temperature ZnO microwire gas sensor through a combined technology of surface etching and UV illumination, *Mater. Lett.* 212 (2) (2018) 296–298.
- [34] A. Runa, X. Zhang, G. Wen, B. Zhang, W. Fu, H. Yang, Actinomorphic flower-like n-ZnO/p-ZnFe2O4 composite and its improved NO₂ gas-sensing property, *Mater. Lett.* 225 (2018) 73–76.
- [35] R. Gao, Z. Ying, W. Sheng, P. Zheng, Gas sensors based on ZnO/silk fibroin film for nitrogen dioxide detection under UV light at room temperature, *Mater. Lett.* 229 (2018) 210–212.
- [36] C.A. Betty, K. Sehra, K.C. Barick, S. Choudhury, Facile preparation of Silicon/ZnO thin film heterostructures and ultrasensitive toxic gas sensing at room temperature: substrate dependence on specificity, *Anal. Chim. Acta* 1039 (2018) 82–90.
- [37] R. Kumar, N. Goel, A.V. Agrawal, R. Raliya, S. Rajamani, G. Gupta, P. Biswas, M. Kumar, M. Kumar, Boosting sensing performance of vacancy-containing vertically aligned MoS₂ using rGO particles, *IEEE Sens. J.* 1748 (c) (2019), pp. 1–1.
- [38] H. Long, A. Harley-Trochimczyk, T. Pham, Z. Tang, T. Shi, A. Zettl, C. Carraro, M.A. Worsley, R. Maboudian, High surface area MoS₂/graphene hybrid aerogel for ultrasensitive NO₂ detection, *Adv. Funct. Mater.* 26 (28) (2016) 5158–5165.
- [39] P.V. Sarma, C.S. Tiwary, S. Radhakrishnan, P.M. Ajayan, M.M. Shajumon, Oxygen incorporated WS₂ nanoclusters with superior electrocatalytic properties for hydrogen evolution reaction, *Nanoscale* 10 (20) (2018) 9516–9524.
- [40] J. Mei, Y. Zhang, T. Liao, Z. Sun, S.X. Dou, Strategies for improving the lithium-storage performance of 2D nanomaterials, *Natl. Sci. Rev.* 5 (3) (2018) 389–416.
- [41] H. Schmidt, F. Giustiniano, G. Eda, Electronic transport properties of transition metal dichalcogenide field-effect devices: surface and interface effects, *Chem. Soc. Rev.* 44 (21) (2015) 7715–7736.

- [42] H. Jin, C. Zhao, R. Gui, X. Gao, Z. Wang, Reduced graphene oxide/nile blue/gold nanoparticles complex-modified glassy carbon electrode used as a sensitive and label-free aptasensor for ratiometric electrochemical sensing of dopamine, *Anal. Chim. Acta* 1025 (2018) 154–162.
- [43] P. Wiench, Z. González, R. Menéndez, B. Grzyb, G. Gryglewicz, Beneficial impact of oxygen on the electrochemical performance of dopamine sensors based on N-doped reduced graphene oxides, *Sens. Actuators B Chem.* 257 (2018) 143–153.
- [44] C. Zhao, et al., Facile synthesis of SnO₂hierarchical porous nanosheets from graphene oxide sacrificial scaffolds for high-performance gas sensors, *Sens. Actuators B Chem.* 258 (2018) 492–500.
- [45] H. Mahmood, L. Vanzetti, M. Bersani, A. Pegoretti, Mechanical properties and strain monitoring of glass-epoxy composites with graphene-coated fibers, *Compos. Part A Appl. Sci. Manuf.* 107 (2018) 112–123.
- [46] J. Hao, L. Ji, K. Wu, N. Yang, Electrochemistry of ZnO@reduced graphene oxides, *Carbon N. Y.* 130 (2018) 480–486.
- [47] X. Yan, et al., Morphology-controlled synthesis of Bi₂S₃ nanorods-reduced graphene oxide composites with high-performance for electrochemical detection of dopamine, *Sens. Actuators B Chem.* 257 (2018) 936–943.
- [48] J. Kong, Nanotube molecular wires as chemical sensors, *Science* 287 (5453) (2000) 622–625 (80-).
- [49] D. Kumar, et al., Effect of single wall carbon nanotube networks on gas sensor response and detection limit, *Sens. Actuators B Chem.* 240 (2017) 1134–1140.
- [50] S.W. Lee, W. Lee, Y. Hong, G. Lee, D.S. Yoon, Recent advances in carbon material-based NO₂ gas sensors, *Sens. Actuators B Chem.* 255 (2) (2018) 1788–1804.
- [51] S.-W. Choi, J. Kim, Y.T. Byun, Highly sensitive and selective NO₂ detection by Pt nanoparticles-decorated single-walled carbon nanotubes and the underlying sensing mechanism, *Sens. Actuators B Chem.* 238 (Jan. 2017) 1032–1042.
- [52] Q.T. Minh Nguyen, et al., Superior enhancement of NO₂gas response using n-p-n transition of carbon nanotubes/SnO₂nanowires heterojunctions, *Sens. Actuators B Chem.* 238 (2) (2017) 1120–1127.
- [53] S. Kumar, V. Pavelyev, P. Mishra, N. Tripathi, A review on chemiresistive gas sensors based on carbon nanotubes: device and technology transformation, *Sens. Actuators A Phys.* 283 (2018) 174–186.
- [54] Y.H. Navale, et al., Zinc oxide hierarchical nanostructures as potential NO₂ sensors, *Sens. Actuators B Chem.* 251 (2) (2017) 551–563.
- [55] Z. Zhang, et al., Novel SnO₂@ZnO hierarchical nanostructures for highly sensitive and selective NO₂ gas sensing, *Sens. Actuators B Chem.* 257 (2018) 714–727.
- [56] X. Sui, C. Hong, W. Pang, C. Chen, Unsymmetrical α -diimine palladium catalysts and their properties in olefin (co)polymerization, *Mater. Chem. Front.* 1 (5) (2017) 967–972.
- [57] N. Karmakar, et al., Room temperature NO₂ gas sensing properties of p-toluenesulfonic acid doped silver-polypyrrole nanocomposite, *Sens. Actuators B Chem.* 242 (2) (2017) 118–126.
- [58] Y. Zhou, G. Liu, X. Zhu, Y. Guo, Ultrasensitive NO₂ gas sensing based on rGO/MoS₂ nanocomposite film at low temperature, *Sens. Actuators B Chem.* 251 (2) (2017) 280–290.
- [59] T. Xu, et al., The ultra-high NO₂ response of ultra-thin WS₂ nanosheets synthesized by hydrothermal and calcination processes, *Sens. Actuators B Chem.* 259 (2) (2018) 789–796.
- [60] Z. Wang, et al., Rational synthesis of molybdenum disulfide nanoparticles decorated reduced graphene oxide hybrids and their application for high-performance NO₂ sensing, *Sens. Actuators B Chem.* 260 (2) (2018) 508–518.
- [61] Y. Li, et al., Hierarchical hollow MoS₂ microspheres as materials for conductometric NO₂ gas sensors, *Sens. Actuators B Chem.* 282 (November 2018) (2019) 259–267.
- [62] Q. Lu, Y. Yu, Q. Ma, B. Chen, H. Zhang, 2D transition-metal-dichalcogenide-nanosheet-based composites for photocatalytic and electrocatalytic hydrogen evolution reactions, *Adv. Mater.* 28 (10) (2016) 1917–1933.
- [63] Y. Shi, H. Li, L.J. Li, Recent advances in controlled synthesis of two-dimensional transition metal dichalcogenides via vapour deposition techniques, *Chem. Soc. Rev.* 44 (9) (2015) 2744–2756.
- [64] Y. Wang, et al., Strain-induced direct-indirect bandgap transition and phonon modulation in monolayer WS₂, *Nano Res.* 8 (8) (2015) 2562–2572.
- [65] A. Ambrosi, M. Pumera, Electrochemical exfoliation of MoS₂ crystal for hydrogen electrogeneration, *Chem. Eur. J.* (2018) 18551–18555.
- [66] A. Ambrosi, Z. Sofer, M. Pumera, Lithium intercalation compound dramatically influences the electrochemical properties of exfoliated MoS₂, *Small* 11 (5) (2015) 605–612.
- [67] T.A. Shifa, et al., Engineering the electronic structure of 2D WS₂ nanosheets using Co incorporation as Cox W(1-x) S₂ for conspicuously enhanced hydrogen generation, *Small* 12 (28) (2016) 3802–3809.
- [68] C.C. Cheng, et al., Activating basal-plane catalytic activity of two-dimensional MoS₂monolayer with remote hydrogen plasma, *Nano Energy* 30 (2016) 846–852.
- [69] G. Zhao, P. Li, K. Rui, Y. Chen, S.X. Dou, W. Sun, CoSe₂/MoSe₂ heterostructures with enriched water adsorption/dissociation sites towards enhanced alkaline hydrogen evolution reaction, *Chem. Eur. J.* 24 (43) (2018) 11158–11165.
- [70] J. Luxa, V. Mazánek, D. Bouša, D. Sedmidubský, M. Pumera, Z. Sofer, Graphene-amorphous transition-metal chalcogenide (MoS_x, WS_x) composites as highly efficient hybrid electrocatalysts for the hydrogen evolution reaction, *ChemElectroChem* 3 (4) (2016) 565–571.
- [71] S. Pourbeyram, J. Abdollahpour, M. Soltanpour, Green synthesis of copper oxide nanoparticles decorated reduced graphene oxide for high sensitive detection of glucose, *Mater. Sci. Eng. C* 94 (October 2018) (2019) 850–857.
- [72] V. Kumar, et al., Enhanced electron transfer mediated detection of hydrogen peroxide using a silver nanoparticle-reduced graphene oxide-polyaniline fabricated electrochemical sensor, *RSC Adv.* 8 (2) (2018) 619–631.
- [73] Z. Li, Y. Liu, D. Guo, J. Guo, Y. Su, Room-temperature synthesis of CuO/reduced graphene oxide nanohybrids for high-performance NO₂ gas sensor, *Sens. Actuators B Chem.* 271 (October 2017) (2018) 306–310.
- [74] C.-S. Lee, S. Yu, T. Kim, One-step electrochemical fabrication of reduced graphene oxide/gold nanoparticles nanocomposite-modified electrode for simultaneous detection of dopamine, ascorbic acid, and uric acid, *Nanomaterials* 8 (1) (2017) 17.
- [75] P. Bollella, et al., Beyond graphene: electrochemical sensors and biosensors for biomarkers detection, *Biosens. Bioelectron.* 89 (2017) 152–166.
- [76] C. Tan, Z. Lai, H. Zhang, Ultrathin two-dimensional multinary layered metal chalcogenide nanomaterials, *Adv. Mater.* 29 (37) (2017) 1–25.
- [77] C. Tan, et al., Preparation of high-percentage 1T-phase transition metal dichalcogenide nanodots for electrochemical hydrogen evolution, *Adv. Mater.* 30 (9) (2018) 1–9.
- [78] Z. Wang, B. Mi, Environmental applications of 2D molybdenum disulfide (MoS₂) nanosheets, *Environ. Sci. Technol.* 51 (15) (2017) 8229–8244.
- [79] M. Donarelli, L. Ottaviano, “2D materials for gas sensing applications: a review on graphene oxide, MoS₂, WS₂ and phosphorene, *Sensors* 18 (11) (2018).
- [80] B. Cho, et al., Metal decoration effects on the gas-sensing properties of 2D hybrid-structures on flexible substrates, *Sensors* 15 (10) (2015) 24903–24913.
- [81] C. Liu, B. L. Chen, G. Liu, A.N. Abbas, M. Fathi, Zhou, High-performance chemical sensing using Schottky-contacted chemical vapor deposition grown monolayer MoS₂ transistors, *ACS Nano* 8 (5) (2014) 5304–5314.
- [82] Y. Niu, R. Wang, W. Jiao, G. Ding, L. Hao, F. Yang, MoS₂ graphene fiber based gas sensing devices, *Carbon N. Y.* 95 (2) (2015) 34–41.
- [83] Y. Dan, Y. Lu, N.J. Kybert, Z. Luo, A.T.C. Johnson, Intrinsic response of graphene vapor sensors, *Nano Lett.* 9 (4) (2009) 1472–1475.
- [84] H. Li, et al., “Fabrication of single- and multilayer MoS₂ film-based field-effect transistors for sensing NO at room temperature, *Small* 8 (1) (2012) 63–67.
- [85] G. Lu, L.E. Ocola, J. Chen1, Gas detection using low-temperature reduced graphene oxide sheets, *Appl. Phys. Lett.* 94 (2009), 083111.
- [86] T. Xu, et al., High-response NO₂ resistive gas sensor based on bilayer MoS₂ grown by a new two-step chemical vapor deposition method, *J. Alloy. Comp.* 725 (2) (2017) 253–259.
- [87] B. Cho, et al., Chemical sensing of 2D graphene/MoS₂ heterostructure device, *ACS Appl. Mater. Interfaces* 7 (30) (2015) 16775–16780.
- [88] P. Preziosi, Stefano Francesco, et al., Graphene oxide as a practical solution to high sensitivity gas sensing, *J. Phys. Chem. C* 117 (20) (2013) 10683–10690.
- [89] S. Shao, L. Che, Y. Chen, M. Lai, S. Huang, R. Koehn, A novel RGO-MoS₂-CdS nanocomposite film for application in the ultrasensitive NO₂ detection, *J. Alloy. Comp.* 774 (2) (2019) 1–10.
- [90] J. Guo, R. Wen, J. Zhai, Z. Lin, Enhanced NO₂ gas sensing of a single-layer MoS₂ by photogating and piezo-phototronic effects, *Sci. Bull.* 64 (2019) 128–135.
- [91] R. Kumar, N. Goel, M. Kumar, UV-activated MoS₂ based fast and reversible NO₂ sensor at room temperature, *ACS Sens.* 2 (11) (2017) 1744–1752.
- [92] M. Kumar, Rahul Kumar, Neeraj Goel, High performance NO₂ sensor using MoS₂ nanowires network, *Appl. Phys. Lett.* 112 (5) (2018), 053502.
- [93] Y.G. Yong Zhou, Cheng Zou, Xiaogang Lin, UV light activated NO₂ gas sensing based on Au nanoparticles decorated few-layer MoS₂ thin film at room temperature, *Appl. Phys. Lett.* 113 (8) (2018), 082103.
- [94] A. Agrawal, R. Kumar, S. Venkatesan, A. Zakhidov, G. Yang, J. Bao, M. Kumar, M. Kumar, Photo-activated mixed in-plane and edge-enriched p-type, *ACS Sens.* 3 (5) (2018) 998–1004.
- [95] Y. Han, et al., Design of hetero-nanostructures on MoS₂ nanosheets to boost NO₂ room-temperature sensing, *ACS Appl. Mater. Interfaces* 10 (26) (2018) 22640–22649.
- [96] J.Z. Ou, et al., Physisorption-based charge transfer in two-dimensional SnS₂ for selective and reversible NO₂ gas sensing, *ACS Nano* 9 (10) (2015) 10313–10323.
- [97] R. Kumar, N. Goel, M. Mishra, G. Gupta, M. Fanetti, M. Valant, “Growth of MoS₂ – MoO₃ hybrid microflowers via controlled vapor transport process for efficient gas sensing at room temperature, *Adv. Mater. Interfaces* 5 (10) (2018) 1800071.
- [98] R. Kumar, P. Kulriya, M. Mishra, F. Singh, G. Gupta, M. Kumar, Highly selective and reversible NO₂ gas sensor using vertically aligned MoS₂ flake networks, *Nanotechnology* 29 (46) (2018) 464001.
- [99] U.A. Mos, et al., Charge-transfer-based gas Sensing Using atomic-layer MoS₂, *Sci. Rep.* 5 (2015) 8052.
- [100] A.Y. Polyakov, et al., Gold decoration and photoresistive response to nitrogen dioxide of WS₂ nanotubes, *Chem. Eur. J.* 24 (71) (2018) 18952–18962.
- [101] M. Ma, et al., A novel wireless gas sensor based on LTCC technology, *Sens. Actuators B Chem.* 239 (2017) 711–717.
- [102] J.Z. Ou, et al., Physisorption-based charge transfer in two-dimensional SnS₂ for selective and reversible NO₂ gas sensing, *ACS Nano* 9 (10) (2015) 10313–10323.
- [103] H. Khan, et al., Quasi physisorptive two dimensional tungsten oxide nanosheets with extraordinary sensitivity and selectivity to NO₂, *Nanoscale* 9 (48) (2017) 19162–19175.
- [104] C. Wang, X. Li, C. Feng, Y. Sun, G. Lu, Nanosheets assembled hierarchical flower-like WO₃ nanostructures: synthesis, characterization, and their gas sensing properties, *Sens. Actuators B Chem.* 210 (2015) 75–81.
- [105] L. Fan, B. Zhu, P.C. Su, C. He, Nanomaterials and technologies for low temperature solid oxide fuel cells: recent advances, challenges and opportunities, *Nano Energy* 45 (October 2017) (2018) 148–176.

- [106] G. Korotcenkov, Gas response control through structural and chemical modification of metal oxide films: state of the art and approaches, *Sens. Actuators B Chem.* 107 (1) (2005) 209–232. SPEC. ISS.
- [107] C. Li, Z. Luo, T. Wang, J. Gong, Surface, bulk, and interface: rational design of hematite architecture toward efficient photo-electrochemical water splitting, *Adv. Mater.* 30 (30) (2018) 1–23.
- [108] M.D. Regalacio, Y. Wang, Z.W. Seh, M.-Y. Han, Tailoring porosity in copper-based multinary sulfide nanostructures for energy, biomedical, catalytic, and sensing applications, *ACS Appl. Nano Mater.* 1 (7) (2018) 3042–3062.
- [109] M. Bao, et al., “Plate-like p-n heterogeneous NiO/WO₃ nanocomposites for high performance room temperature NO₂ sensors, *Nanoscale* 6 (2014) 4063–4066.
- [110] X. Chen, et al., In-situ growth of ZnO nanowire arrays on the sensing electrode via a facile hydrothermal route for high-performance NO₂sensors, *Appl. Surf. Sci.* 435 (2) (2018) 1096–1104.
- [111] K. Diao, J. Xiao, Z. Zheng, X. Cui, Enhanced sensing performance and mechanism of CuO nanoparticle-loaded ZnO nanowires: comparison with ZnO-CuO core-shell nanowires, *Appl. Surf. Sci.* 459 (July) (2018) 630–638.
- [112] L. Qi, L. Yu, Z. Liu, F. Guo, X. Fan, An enhanced optoelectronic NO₂ gas sensors based on direct growth ZnO nanowalls in situ on porous rGO, *J. Alloy. Comp.* 749 (2) (2018) 244–249.
- [113] S. Liu, B. Yu, H. Zhang, T. Fei, T. Zhang, Enhancing NO₂ gas sensing performances at room temperature based on reduced graphene oxide-ZnO nanoparticles hybrids, *Sens. Actuators B Chem.* 202 (2) (2014) 272–278.
- [114] G. Lu, J. Xu, J. Sun, Y. Yu, Y. Zhang, F. Liu, UV-enhanced room temperature NO₂ sensor using ZnO nanorods modified with SnO₂ nanoparticles, *Sens. Actuators B Chem.* 162 (1) (2012) 82–88.
- [115] C. Manh, H. Viet, N. Van Duy, N. Duc, Comparative effects of synthesis parameters on the NO₂ gas-sensing performance of on-chip grown ZnO and Zn₂SnO₄ nanowire sensors, *J. Alloy. Comp.* 765 (2) (2018) 1237–1242.
- [116] X. Chen, et al., Synthesis of ZnO nanowires/Au nanoparticles hybrid by a facile one- pot method and their enhanced NO₂ sensing properties, *J. Alloy. Comp.* 783 (2019) 503–512.
- [117] S. Bai, et al., Reverse microemulsion in situ crystallizing growth of ZnO nanorods and application for NO₂ sensor, *Sens. Actuators B Chem.* 190 (2014) 760–767.
- [118] J. Lee, A. Katoch, J. Kim, S.S. Kim, Effect of Au nanoparticle size on the gas-sensing performance of p-CuO nanowires, *Sens. Actuators B Chem.* 222 (2016) 307–314.
- [119] Y.H. Navale, S.T. Navale, F.J. Stadler, N.S. Ramgir, V.B. Patil, Enhanced NO₂ sensing aptness of ZnO nanowire/CuO nanoparticle heterostructure-based gas sensors, *Ceram. Int.* 45 (2) (2019) 1513–1522.
- [120] Q. Zhang, et al., Visible light-assisted room temperature gas sensing with ZnO-Ag heterostructure nanoparticles, *Sens. Actuators B Chem.* 259 (2018) 269–281.
- [121] Z. Liu, et al., Facial development of high performance room temperature NO₂gas sensors based on ZnO nanowalls decorated rGO nanosheets, *Appl. Surf. Sci.* 423 (2017) 721–727.
- [122] S.K. Shaikh, V.V. Ganbavale, S.V. Mohite, U.M. Patil, K.Y. Rajpure, ZnO nanorod based highly selective visible blind ultra-violet photodetector and highly sensitive NO₂ gas sensor, *Superlattice Microstruct.* 120 (May) (2018) 170–186.
- [123] W. Chebil, et al., Structural, optical and NO₂ gas sensing properties of ZnMgO thin films prepared by the sol gel method, *Phys. B Phys. Condens. Matter* 505 (2) (2017) 9–16.
- [124] N.B. Patil, A.R. Nimbalkar, M.G. Patil, ZnO thin film prepared by a sol-gel spin coating technique for NO₂ detection, *Mater. Sci. Eng. B* 227 (2) (2018) 53–60.
- [125] Y. Yang, H.E. Katz, “Hybrid of P3HT and ZnO @ GO nanostructured particles for increased NO₂ sensing response †, *J. Mater. Chem. C* 5 (2017) 2160–2166.
- [126] Q. Li, Y. Cen, J. Huang, X. Li, H. Zhang, Y. Geng, Zinc oxide – black phosphorus composites for ultrasensitive nitrogen dioxide sensing †, *Nanoscale Horiz.* 3 (2018) 525–531.
- [127] S.A. Vanalakar, M.G. Gang, V.L. Patil, T.D. Dongale, Enhanced gas-sensing response of zinc oxide nanorods synthesized via hydrothermal route for nitrogen dioxide gas, *J. Electron. Mater.* 48 (1) (2019) 589–595.
- [128] A. Aziz, N. Tiwale, S.A. Hodge, S. Attwood, G. Divitini, M.E. Welland, Core-shell electrospun polycrystalline ZnO nanofibres for ultra-sensitive NO₂ gas sensing, *ACS Appl. Mater. Interfaces* 10 (50) (2018) 43817–43823.
- [129] R. Chen, J. Wang, L. Xiang, Facile synthesis of mesoporous ZnO sheets assembled by small nanoparticles for enhanced NO₂ sensing performance at room temperature, *Sens. Actuators B Chem.* 270 (2018) 207–215.
- [130] S. Bok, C. Woo, S. Lee, C. Lee, S. Lee, Enhanced NO₂ gas-sensing performance of Pd/ZnO-decorated SnO₂ nanorod sensors, *Appl. Phys. A* 124 (12) (2018) 1–9.
- [131] Jyoti, G.D. Varma, Synthesis of CuO-ZnO/rGO ternary composites for superior NO₂ gas sensor at room temperature, *Mater. Res. Express* 6 (3) (2018), 035011.
- [132] D. Han, L. Zhai, F. Gu, Z. Wang, Highly sensitive NO₂ gas sensor of ppb-level detection based on in 2 O 3 nanobricks at low temperature, *Sens. Actuators B Chem.* 262 (2) (2018) 655–663.
- [133] X. Li, et al., Vitamin C-assisted synthesis and gas sensing properties of coaxial in 2 O 3 nanorod bundles, *Sens. Actuators B Chem.* 220 (2015) 68–74.
- [134] J. M, G.L. Qiuyue Yang, Xiaobiao Cui, Jiangyang Liu, Jing Zhao, Yinglin Wang, Yuan Gao, Peng Sun, A low temperature operating gas sensor with high response to NO₂ based on ordered mesoporous, *New J. Chem.* 40 (2016) 2376–2382.
- [135] B. Xiao, Q. Zhao, D. Wang, M. Zhang, Facile synthesis of nanoparticle packed in 2 O 3 nanospheres for highly sensitive NO₂ sensing, *New J. Chem.* 41 (16) (2017) 8530–8535.
- [136] C. Woong, et al., Highly selective and sensitive detection of NO₂ using rGO-In 2 O 3 structure on flexible substrate at low temperature, *Sens. Actuators B Chem.* 255 (2) (2018) 1671–1679.
- [137] Z. Wang, et al., The enhanced NO₂ sensing properties of SnO₂ nanoparticles/reduced graphene oxide composite, *J. Colloid Interface Sci.* 537 (2) (2019) 228–237.
- [138] G. Neri, A. Bonavita, G. Micali, G. Rizzo, E. Callone, G. Carturan, Resistive CO gas sensors based on In₂O₃ and InSnO_x nanopowders synthesized via starch-aided sol-gel process for automotive applications, *Sens. Actuators B Chem.* 132 (1) (2008) 224–233.
- [139] R. You, D.D. Han, F. Liu, Y.L. Zhang, G. Lu, Fabrication of flexible room-temperature NO₂ sensors by direct laser writing of In₂O₃ and graphene oxide composites, *Sens. Actuators B Chem.* 277 (2) (2018) 114–120.
- [140] W. Yang, P. Wan, X. Zhou, J. Hu, Y. Guan, L. Feng, Additive-free synthesis of In₂O₃ cubes embedded into graphene sheets and their enhanced NO₂ sensing performance at room temperature, *ACS Appl. Mater. Interfaces* 6 (23) (2014) 21093–21100.
- [141] H.Y. Lee, Y.C. Heish, C.T. Lee, High sensitivity detection of nitrogen oxide gas at room temperature using zinc oxide-reduced graphene oxide sensing membrane, *J. Alloy. Comp.* 773 (2019) 950–954.
- [142] T. Han, S. Gao, Z. Wang, T. Fei, S. Liu, T. Zhang, Investigation of the effect of oxygen-containing groups on reduced graphene oxide-based room-temperature NO₂ sensor, *J. Alloy. Comp.* 801 (2019) 142–150.
- [143] H. Yan, et al., Effects of the oxidation degree of graphene oxide on the adsorption of methylene blue, *J. Hazard Mater.* 268 (2014) 191–198.
- [144] D.C. Marcano, D.V. Kosynkin, J.M. Berlin, A. Sünitskii, Z. Sun, A. Slesarev, et al., Improved synthesis of graphene oxide, *ACS Nano* 4 (2010) 4806–4814.
- [145] A. Giampiccolo, et al., Sol gel graphene/TiO₂ nanoparticles for the photocatalytic-assisted sensing and abatement of NO₂, *Appl. Catal. B Environ.* 243 (October 2018) (2019) 183–194.
- [146] J. Cha, S. Choi, I. Kim, 2D WS₂-edge functionalized multi-channel carbon nanofibers: effect of WS₂ edge-abundant structure on room temperature NO₂ sensing, *J. Mater. Chem. 5* (18) (2017) 8725–8732.
- [147] S. Zhao, Z. Li, G. Wang, J. Liao, S. Lv, Z. Zhu, Highly enhanced response of MoS₂/porous silicon nanowire heterojunctions to NO₂ at room, *RSC Adv.* 8 (2018) 11070–11077.
- [148] X. Li, J. Wang, D. Xie, J. Xu, Y. Xia, L. Xiang, Enhanced p-type NO₂-sensing properties of ZnO nanowires utilizing CNTs electrode 206 (Nov. 2017) 18–21.
- [149] J. Kim, J. Lee, A. Mirzaei, H. Woo, S. Sub, SnO₂ (n) -NiO (p) composite nanowebs : gas sensing properties and sensing mechanisms, *Sens. Actuators B Chem.* 258 (2018) 204–214.
- [150] H. Lee, Y. Heish, C. Lee, High sensitivity detection of nitrogen oxide gas at room temperature using zinc oxide-reduced graphene oxide sensing membrane, *J. Alloy. Comp.* 773 (2019) 950–954.
- [151] A.R. Nimbalkar, N.B. Patil, V.V. Ganbavle, S.V. Mohite, K.V. Madhale, M.G. Patil, Sol-gel derived aluminium doped zinc oxide thin films : a view of aluminium doping effect on physicochemical and NO₂ sensing properties, *J. Alloy. Comp.* 775 (2) (2019) 466–473.
- [152] A. You, M.A.Y. Be, I. In, Multi-layered zinc oxide-graphene composite thin films for selective nitrogen dioxide sensing, *J. Appl. Phys.* 084501 (November 2017) (2018).
- [153] Lalit Chandra, R. Dwivedi, V.N. Mishra, Highly sensitive NO₂ sensor using brush-coated ZnO nanoparticles, *Mater. Res. Express* 4 (2017) 105030.